

Self-learning Machines based on Hamiltonian Echo Backpropagation

Victor Lopez-Pastor¹ and Florian Marquardt^{1,2}

¹Max Planck Institute for the Science of Light, Erlangen, Germany

²Physics Department, Friedrich-Alexander-Universität Erlangen-Nürnberg, Erlangen, Germany

(Dated: March 8, 2021)

A physical self-learning machine can be defined as a nonlinear dynamical system that can be trained on data (similar to artificial neural networks), but where the update of the internal degrees of freedom that serve as learnable parameters happens autonomously. In this way, neither external processing and feedback nor knowledge of (and control of) these internal degrees of freedom is required. We introduce a general scheme for self-learning in any time-reversible Hamiltonian system. We illustrate the training of such a self-learning machine numerically for the case of coupled nonlinear wave fields.

I. INTRODUCTION

In the last decade, the field of Machine Learning (ML) has experienced an explosive growth, finding use in an ever-increasing number of applications in our everyday lives, from automatic driving to face recognition. To a large degree, this astonishing progress in ML can be attributed to the developments in Artificial Neural Networks (ANN). Training deep ANN's has only recently become possible in practice [1], thanks both to the availability of large data sets and to the continued improvement in digital electronic hardware and the advent of fast Graphical Processing Units (GPU) and other specialized hardware. However, while the demand for faster and more efficient information processing will only grow in order to address the needs of increasingly larger and complex ANN's, the exponential growth in the power of electronic devices that we enjoyed in the last half century appears to be coming to a halt.

What is more, the von Neumann architecture that is currently employed by electronic devices is known to be highly inefficient for most ML applications. In a von Neumann computer, the memory and processing units are separated, and the necessary transfer of data between them can severely constrain the overall performance. The field of *neuromorphic computing* [2] aims to improve the efficiency of specialized hardware for ML by imitating the structure of biological neural networks. The hope is to realize devices that are as efficient and massively parallel as the brain, while using much faster physical processes to carry out the information processing.

In particular, the idea of constructing neuromorphic computing devices based on light has recently attracted a lot of attention, as it promises to unlock all the benefits of optical computing: broad bandwidth, small latency, low power consumption and natural parallelism [3]. Apart from optics, other physical platforms have been considered too, such as spin-based devices or memristor circuits [2].

Nonetheless, *training* such machines is still a challenging problem. The best solution would be to realize a *self-learning machine* - i.e. a learning machine that is trained by means of entirely autonomous physical pro-

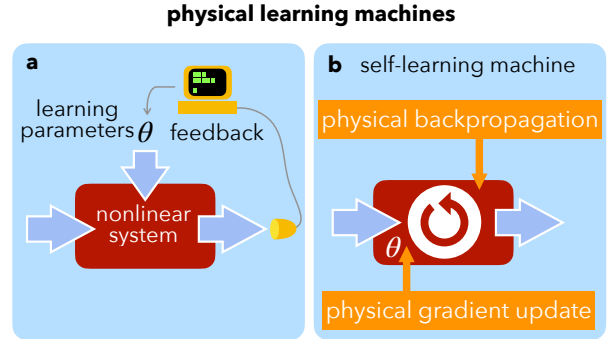


Figure 1. **Different types of physical learning machines.** (a) Physical learning machine requiring feedback based on the outcome, to tune the internal "learning" parameters θ inside the physical device. (b) A self-learning machine does not involve feedback. It updates the learning parameters in a fully autonomous way (for example using physical backpropagation and a physical gradient update; see main text).

cesses (Fig. 1), without the use of feedback for updating the learning parameters and without any kind of external processing of information (except possibly that needed for feeding the training data). A first step in this direction was already suggested theoretically in a visionary paper by Psaltis et al. [4] and later implemented to some degree [5]. In that paper, it was shown that it could be possible to approximately realize the backpropagation algorithm [6] in an optical neural network based on volume holograms. However, the nonlinear elements must be engineered so that the transmittance for the backpropagating signal matches the derivative of the transmittance for the forward propagating signal, besides requiring a carefully designed geometric arrangement [7]. To this day, such stringent requirements have prevented a fully developed practical implementation of the backpropagation algorithm in an optical learning machine [8].

Other learning machines based on Hebbian learning or Spiking Timing-Dependent Synaptic Plasticity (STDSP) would also fall under our definition of a self-learning machine [9]. Still, both Hebbian learning and STDSP are motivated mainly by their plausibility in the context of biological neural networks. Unlike the methods based on

the optimization of a cost function, their use most often lacks a rigorous mathematical foundation, and their performance is typically poor when applied to deep learning tasks.

In this work we consider SL machines based on classical Hamiltonian systems. We present a new training procedure based on time reversal operations, which we name Hamiltonian Echo Backpropagation (HEB). As opposed to existing approaches, we do not need to consider a particular implementation of a SL machine or carefully selected nonlinear elements; instead we present a completely general procedure to train SL machines in a wide class of physical systems. Indeed, HEB can realize gradient descent and update of the learning parameters via the dynamics in *any* time-reversible Hamiltonian system, and it does so in an efficient way that exploits the parallelism of the learning machine. This new training procedure opens up many exciting possibilities, making it possible to construct self-learning machines in a wide range of physical platforms. On the one hand, HEB makes it feasible to realize SL devices based on already mature technologies, such as integrated photonic circuits. On the other hand, it expands the field of SL machines to new interesting physical platforms, such as clouds of cold atoms or trains of optical pulses in a fiber loop. Given how broad are the sufficient conditions for HEB to work, we believe that it will instigate the discovery of completely new physical learning machines. Moreover, our training procedure is independent of the Hamiltonian that describes the dynamics of the learning machine. Surprisingly, one does not even need to know the dynamics of the physical device in order to train it.

In the following, after defining self-learning machines, we will introduce the Hamiltonian Echo Backpropagation procedure and present a mathematical proof of its core element. We will then discuss the ingredients of such a machine, illustrate the learning approach in two numerical examples, and finally comment on the prospects for different physical platforms.

II. SELF-LEARNING MACHINES

Definitions: Physical learning machines vs. physical self-learning machines

A *physical learning machine* can be defined as a physical device provided with an internal memory that can process an input to produce an output, such that the functional dependence between the input and the output is parameterized by the state of the internal memory. For example, a physical learning machine can be a photonic circuit made of beam-splitters, nonlinear elements and variable phase shifters. In this example, for any input signal that enters the circuit, the output will depend on the configuration of the phase shifters, which in this case represent the internal memory. In a physical learning machine, training is the process of finding

the optimal state of the internal memory to realize some desired input-output relation.

There are several possible ways of training a physical learning machine. It could be done entirely externally (using numerical simulations) or by employing feedback, i.e. external processing of the machine's output to adapt the parameters. However, this step may spoil some of the advantages of using physical dynamics. Going beyond that, the most advanced version would consist in a machine that uses an internal physical process for training. We may thus define a *self-learning machine* as a physical learning machine that, when presented a data set, can train itself in a fully autonomous way. During training, a self-learning machine receives a sequence of inputs and some information about the target outputs. It is also legitimate to realize a preset sequence of external operations on the SL machine or to supply energy. What is not permissible is to give any kind of feedback dependent on the internal state of the device. In this sense, a SL machine is a black box: the user provides an input and obtains an output, but requires neither knowledge of nor access to the internal degrees of freedom.

Optimization vs. Heuristic approaches

Apart from the distinction between non-autonomous and autonomous (self-learning) machines, we may also classify the training of physical learning machines along another axis, subdividing them into two broad classes, the *heuristic* approaches and schemes based on *optimization*.

A broad category of devices makes use of learning rules inspired by biological neural networks. We call this set of ideas the *heuristic* approach. This corpus of ideas started historically with Hebbian learning and it can be summarized in the motto 'neurons that fire together, wire together'. A more sophisticated version in the context of spiking neurons is the so-called spike-timing-dependent synaptic plasticity. Importantly, these learning rules are always local in order to be biologically plausible (i.e. the update in the learning parameters is a function of only the nearest neighbouring neurons). The fact that these training rules are local makes them potentially easier to implement in a physical device.

However, the training rules in the heuristic category often lack a rigorous mathematical foundation. Such a general mathematical foundation does exist for the second set of ideas, which underpin modern machine learning: there, the challenge of training is converted into an *optimization* problem. In this approach, training the learning machine consists in finding the learning parameters that minimize a cost function, which quantifies the deviation between desired output and actual output. Typically, the minimization is done by means of some variant of the gradient descent algorithm. In this article, we will focus entirely on the optimization approach.

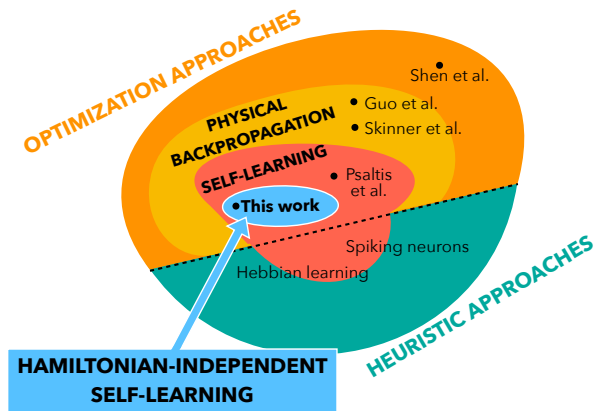


Figure 2. **Overview: The landscape of physical learning machines.** Our work falls into the broad class of optimization approaches. It belongs to the small class of works that involve both physical backpropagation and self-learning, but in contrast to other approaches our scheme is universal, i.e. independent of the specific Hamiltonian. (some related works, see main text: Shen et al [10], Guo et al [11], Skinner et al [12], Psaltis et al [4, 5]).

Review of physical learning machines

The idea of using specialized physical hardware for ML has been explored in various platforms. What we define as physical learning machines have been studied theoretically and for some cases already demonstrated experimentally in the context of photonic hardware [5, 10, 11, 13], memristor circuits [14, 15], and spintronic devices [16, 17], among others. Here we review some of the most relevant ideas on the topic to prepare a comparison with our concept. We focus on optimization approaches and the problem of training.

In some of the earlier attempts [12], training was done *in silico*, by means of numerical simulations. The problem with this approach is that the size of the learning machine is limited by the computational power required to simulate the physical hardware. Moreover, training is performed for an idealized model of the actual physical hardware. As a result, fabrication imperfections cannot be taken into account.

To remedy this shortcoming, one can employ feedback.

The simplest feedback-based training technique uses a finite-difference approximation to the gradient of the cost function. This can be realized physically in a very simple manner: (1) estimate the cost function C for the current state of the learning parameters, (2) change the i -th parameter by a small amount and estimate C again, (3) add the difference of these results to the i -th parameter. That is the approach used in a number of works (e.g. Shen et al. [10]). However, this idea is far from optimal, since the number of evaluations needed scales with the number of parameters.

We know that the backpropagation algorithm that forms the cornerstone of artificial neural network training

can update all the parameters using only two evaluations of the network, independent of the number of parameters. A crucial improvement of a physical learning machine therefore consists in realizing the backpropagation algorithm by physical means. This idea was first introduced in Wagner et al. [4], in the context of optical neural networks. In a typical optical neural network, an optical field propagates inside some nonlinear medium with elements that provide controllable phase shifts. The controllable phase shifts play the role of the learning weights. The optical field would be injected at the input and propagate towards the output. The idea advocated in [4] then is to create a physical *error signal* that propagates in the opposite direction, from output to input. The error signal is prepared according to the difference of the output of the device and the desired target output. Without going into any further detail (we refer to the original paper), in their approach the backward-propagating weak error signal interferes with the strong forward-propagating optical field. In this way, for the specific choice of optical nonlinearities in their setup it was possible to ensure that the error signal is (approximately) equal at any point of the device to the required gradient of the cost function. Once the error signal is prepared, one can measure it and use the result to update the parameters via feedback. All learning parameters could be updated at once, in a fully parallel fashion. This idea was originally proposed for optical neural networks using Kerr nonlinearities [4], but it was recently extended to setups that employ saturable absorption for the activation function [11]. In a similar spirit, in Hermans et al [18], the idea of physical backpropagation is used to train a physical linear system with controllable nonlinear feedback. A related idea by Hughes, Fan et al. [19] uses an auxiliary circuit to backpropagate the error signal.

Nonetheless, there is a potential drawback in using feedback to update the learning parameters. The error signal has to be measured in order to update the learning weights. If that is done by means of electronic sensors, that could potentially introduce a bottleneck. The potential advantage of using ultrafast physical dynamics for evaluating the network could be lost because of a relatively slow electronic response. In addition, some of these approaches require further computation steps. These problems can be addressed if the error signal could directly influence the learning parameters, without external feedback.

The possibility of using a physical mechanism to update the learning parameters autonomously was proposed for the first time also by Wagner and Psaltis [4]. In their paper, they consider a setup in which the learning parameters are recorded in the form of a hologram in a photorefractive material. In this way, the interference between the error signal and the forward-propagating beam could in principle provide the means to update the holographic recording in the right way. A simple version was partially demonstrated in a linear optical device in a follow-up paper by Li, Psaltis et al [13]. However, that experimental

setup did actually still involve some form of feedback.

The ideas advanced in [4] could potentially lead to ultrafast training and a huge density of interconnections between neurons. By combining physical backpropagation with an autonomous process to update the parameters according to the error signal, it would be possible to realize self-learning machines. Nevertheless, all presently existing proposals for physical backpropagation are suitable only for some setups with very specific nonlinearities. In some cases, such as [4] or [11], it is required that the forward propagating beams and the error signal experience a different dynamics at the nonlinear elements, that nonetheless has to be matched in a precise way. What is more, recording the learning parameters in a holographic pattern requires a very careful engineering of the geometry of the device [7]. In other cases, such as [12], physical backpropagation is only realized approximately in a particular limit.

In this work, we show how to realize self-learning (i.e. the combination of physical backpropagation and autonomous parameter update) in a much broader set of physical systems. Since our idea does not rely on a specific choice of the system, it is not restricted to optical setups. Hence, it could be applied to many other possible platforms, ranging from cold atom clouds to solid state spin networks. In fact, the training procedure that we propose is a sequence of operations that do not even depend on the particular dynamics of the device, provided that some weak assumptions are met. Essentially, we only require that the physical learning machine is based on a time-reversible nonlinear Hamiltonian system.

Hamiltonian-independent self-learning

Let us be more precise about the assumptions made in this paper. First of all, we shall remark that we only consider Hamiltonian systems, where the dynamical degrees of freedom consist in the learning parameters and the variables needed to process the information. This is not a very restrictive assumption from the point of view of the functionality of the device. Although most standard architectures for artificial neural networks produce contractive non-Hamiltonian maps, we point out that it is always possible to cast a contractive dynamical system as a Hamiltonian system with the help of extra ancillary degrees of freedom (we explain this idea in more detail in a later section). From the point of view of the physical realization, it means that the timescale of dissipation in the self-learning device must be much larger than the time interval between the injection of the input and the production of the output. Since we aim to use fast dynamical processes, this seems to be a reasonable requirement. In fact, many of the previous proposals for physical learning machines can be modeled as Hamiltonian systems, e.g. the optical neural networks using Kerr nonlinearity.

The second assumption is that the self-learning device

has time-reversal symmetry. The first main contribution of this paper is a new method to realize physical backpropagation in arbitrary Hamiltonian systems with time-reversal symmetry. This new method is based on a time reversal operation weakly perturbed in a particular way. As a result of this time reversal operation, a perturbed echo is produced inside the device. We show that this echo contains the information needed to update the learning parameters. The echo is used to update the parameters by means of another operation that will be defined later, the *decay step*. We call this method Hamiltonian Echo Backpropagation (HEB).

We summarize the assumptions in our paper in the following two definitions. A Hamiltonian self-learning machine is a self-learning machine that is Hamiltonian and time-reversible. A Hamiltonian-independent self-learning machine is a Hamiltonian self-learning machine in which the training procedure is independent of the Hamiltonian. By this statement, we mean that the training procedure can minimize the cost function for any Hamiltonian that fulfills the two assumptions mentioned above.

To the best of our knowledge, our proposal constitutes the first example of an approach to construct Hamiltonian-independent self-learning machines. Since the training procedure does not depend on the particular form of the Hamiltonian, the self-learning machine can be regarded as a black box. As opposed to other physical learning machines in the literature, its implementation in the laboratory does not even need a detailed knowledge of the internal dynamics of the device in order to make it work. There are only few mechanisms that could disrupt an experimental implementation: a mechanism that in some way breaks time-reversal symmetry of the Hamiltonian (including an unwanted dissipation or noise channel), or significant imperfections in the implementation of the time-reversal operation or the decay step.

In order to realize our proposal in a completely Hamiltonian-independent way, the time reversal and the decay step must be realized outside the device, by means of external operations. For example, this is possible if the SL machine is a photonic circuit and the learning dynamical variables are wave packets that can propagate in and out. However, there are many possible implementations of a SL machine where the time-reversal and decay steps must be performed inside the device. In such cases, we need an additional assumption: the ground state of the Hamiltonian of the device must be continuously degenerate with respect to the learning parameters. This additional requirement seems perhaps quite restrictive. However, as we shall discuss later, the degeneracy can be approximate, provided that the difference in energy between the degenerate minima is small enough. Putting aside the learning parameters, for the rest of the dynamical variables (used to process the information) there is almost absolute freedom in the Hamiltonian, with the only requirement of having time-reversal symmetry and any sort of nonlinear dynamics.

In most of the subsequent discussion, we will analyze our method in the case in which the Hamiltonian possesses a continuously degenerate ground state. Then, in subsection III F we will discuss our approach for the case in which the time reversal operation and the decay step are performed externally. In section IV we will prove that our training method can realize backpropagation exactly in the most general case.

III. HAMILTONIAN ECHO BACKPROPAGATION

A. Dynamical variables and Hamiltonian

Our setup for a SL machine consists of two basic ingredients: dynamical variables that are used to process the information (the *evaluation* variables), and dynamical variables that contain the learning parameters.

The evaluation variables will be combined into a single dynamical vector, $\Psi(t)$. In a similar way, the collection of all the learning parameters is denoted as a vector $\Theta(t)$. Such vectors can represent any collection of physical degrees of freedom in a Hamiltonian system, from interacting spins to optical fields. For the present discussion, we imagine discrete models with a countable number of degrees of freedom. However, the approach also covers the case of continuous fields (with straightforward slight changes in the notation).

The input to the device is given by the initial configuration of the evaluation variables, $\Psi(-T)$, whereas the output is given by its state at a later time, $\Psi(0)$. We choose the initial time to be $-T$ for reasons that will become clear later. The learning parameters, $\Theta(t)$, will interact with the evaluation variables and overall change slowly during training.

For example, consider a self-learning machine where Ψ and Θ are nonlinear wave fields. These could be realized as a lattice of optical cavities or spins. We can imagine the operation of the SL machine as a nonlinear scattering experiment, where the input $\Psi(-T)$ is a wave packet. As the wave packet propagates inside the device, it evolves under the effect of the nonlinear self-interaction and the interaction with the learning parameters. Finally, an output wave packet is obtained at $t = 0$. The output state of Ψ is a nonlinear function of the input, and it has a parametric dependence on the initial configuration of the learning parameters, $\Theta(-T)$, much like an artificial neural network (ANN).

We can capture the dynamics of the SL machine in a single Hamiltonian:

$$H_{SL} = H_{\psi} + H_{int} + H_{\theta} + H_{bath}. \quad (1)$$

Let us inspect one by one what each term means. Some of the technical details will be more fully explained later.

H_{ψ} is the Hamiltonian that describes the evolution of Ψ alone, in the absence of interaction with Θ . In general,

it will have self-interaction (non-quadratic) terms. The second term, H_{int} , contains the interaction of Θ and Ψ . In general, $H_{\psi} + H_{int}$ must be a time-reversible Hamiltonian, but there is no further constraint. In accordance with previous proposals for physical learning machines, we may assume that, for example, Ψ is an optical field inside a nonlinear medium. The nonlinear response of such a medium may correspond, among many other possible choices, to a Kerr-like nonlinearity.

The second term, H_{θ} , describes the dynamics of Θ in the absence of interaction with Ψ . The purpose of Θ is to store the internal degrees of freedom that the SL machine can learn. We need Θ to be able to store information once trained, but it is also important that it can change continuously during training. Hence, we will need to ensure that there is a continuous stable manifold in the phase space of Θ : once the training is finished and Θ converges to some particular point in this stable manifold, it will remain there (at least until it interacts again with Ψ). At the same time, during training the state of Θ can change continuously from one stable point to another in the search of a minimum of the cost function. The interaction between Ψ and Θ may be given by any time-reversible Hamiltonian, but in the absence of interaction we must impose that the dynamics of Θ possesses such a stable manifold.

In the conceptually simplest setup for a SL machine, once the interaction between Ψ and Θ is complete, the dynamics of Θ is just that of a free particle. In this case, the ground state of the Hamiltonian is any configuration with zero momentum: $\pi_{\theta} = 0$. Ideally, any such state is a stable fixed point, and therefore, we can use the parameter Θ as our learning parameter. What our training procedure does is to impart an additional effective force on Θ proportional to the gradient of the cost function. This breaks the degeneracy of H_{θ} , in such a way that the only surviving stable fixed points are the minima of the cost function. But that is not enough to realize training: we not only need to have stable points, we also need a mechanism to converge to them; i.e. we not only require stability, we need asymptotic stability [that is, relaxation towards the fixed points]. That cannot be achieved purely based on Hamiltonian dynamics alone, as we will now discuss.

B. Controllable dissipation

Our training procedure needs both steps with purely Hamiltonian evolution (where we can use time-reversals to our advantage) and steps with dissipative evolution (so that a contractive map on the learning parameters can be realized). This is described by the third term in the Hamiltonian, H_{bath} . This term describes a dissipative bath coupled only to Θ . We further assume that this interaction possesses the same symmetries as H_{θ} . In the example of a free particle Hamiltonian for Θ , this would mean that the joint system of Θ and the thermal reservoir

is invariant with respect to a shift in θ . This assumption is required to ensure that the coupling to the bath does not break the degeneracy. As a result, Θ is subject to dissipation. But at the same time, during our training method we require to be able to perform time reversals. The conceptually simplest way to resolve this conflict is to have the ability to switch dissipation on and off. In principle, we can do so by controlling the coupling of Θ to the reservoir, and many physical implementations (e.g. all approaches related to laser cooling ideas) are possible.

C. Gradient descent as a goal

Suppose that Θ is initialized in some random configuration $\Theta(-T)$. Now, we prepare Ψ in the input state, and we let it interact with Θ . After a time interval T , we will obtain the output state. The error in the output is quantified by means of a cost function. In general, a *cost function* can be any function

$$C(\Psi(0), \Psi_{target}) = C(\Psi(-T), \Psi_{target}, \Theta(-T)) \quad (2)$$

of the output $\Psi(0)$ and its corresponding target configuration that is minimized when both are equal. The function displayed here is the sample-specific cost function. The training procedure will try to minimize its sample-averaged version (averaging over all training input samples $\Psi(-T)$ that are provided alongside their respective target Ψ_{target}). After averaging, the cost function still depends on the learning variables $\Theta(-T)$, since these determine the mapping from input to output.

For reasons that will become apparent later, we take our cost function to have units of energy (and in fact it will represent a physical Hamiltonian later in this section). In order to improve the performance of the SL machine, we have to minimize the cost function. In principle, the problem of optimizing the cost function is a very hard nonlinear optimization problem, but in the context of ML it is usually sufficient to find a local minimum. In the context of ANN's, this is normally done by the stochastic gradient descent method. In this method, the gradient of the cost function is computed (for one or several randomly chosen training samples) and the learning parameters are subsequently updated, according to the rule

$$\theta(T_f) = \theta(-T) - \eta \frac{\partial C}{\partial \theta(-T)}. \quad (3)$$

D. Introducing Hamiltonian Echo Backpropagation

Our goal is to realize the stochastic gradient update rule in a fully autonomous way, via physical dynamics. The sample-specific cost function depends on the output

and the target state. For this reason, if one hopes to implement gradient descent without external intervention, some information about the output must be sent *backwards* from the output to the input. This immediately suggests the use of a time reversal operation, which was already recognized in early proposals [4], although it was employed in a manner different than what we will describe now.

To understand the qualitative idea of our approach, we start from a general observation that is well known from discussions of backpropagation in ANNs. The change of the cost function induced by a small change in a learning parameter θ is given by

$$\delta C = 2\delta\theta Re \left\{ \frac{\partial \Psi(0)}{\partial \theta} \frac{\partial C}{\partial \Psi(0)} \right\} \quad (4)$$

In other words, we need to know both the perturbation in the output configuration $\delta \Psi(0) = \frac{\partial \Psi(0)}{\partial \theta}$ produced by a small parameter change, as well as the "error signal" $\frac{\partial C}{\partial \Psi(0)}$ at the output.

Since we consider weak perturbations, $\delta \Psi(0)$ can be understood in terms of the linear response of the system. In other words, $\delta \Psi(0)$ is in fact proportional to the Green's function associated with the linearized equations of motion. At this point we can introduce the most important idea of our approach: if we physically time-reverse the whole field Ψ , we can instead interpret the error signal, $\frac{\partial C}{\partial \Psi(0)}$ as the source of a perturbation that is "riding on top of" the time-reversed nonlinear wave field (see Fig. 3). This is at the heart of our new procedure to realize self-learning, "Hamiltonian Echo Backpropagation" (HEB).

As we will see later, the idea is related to the fact that in a linear system of differential equations there is a symmetry between the source of a field at t and its effect at t' (the so-called self-reciprocity principle) [?].

Let us go through the individual steps of the HEB procedure. First, Ψ is prepared in the input state, at time $t = -T$. Note that we choose to start the process at time $t = -T$ to make explicit the time-reversal symmetry. Thus, the output is produced at $t = 0$, and the echo of the input will form at $t = T$. In order to simplify the calculations, let us also assume first that the canonical momentum of θ is initially zero. After the interaction between Ψ and Θ , we obtain an output field $\Psi(0)$.

In the next instant, we need a way to inject the error signal required for the subsequent backward pass. This we achieve by imposing on Ψ an interaction Hamiltonian proportional to the (sample-specific) cost function, given the desired target field configuration. We assume that the duration of this interaction, ϵ , is small enough. In practice, this implies that the field is slightly changed according to $\Psi(0) \rightarrow \Psi(0) - i\epsilon \partial_{\Psi^*(0)} C$

Before going further in the discussion of HEB, let us introduce a useful notation we will employ in the rest of the paper. In order to make our equations more compact, we condense each pair of canonical coordinates in a

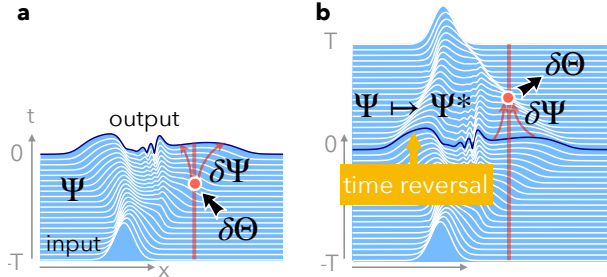


Figure 3. **Physical backpropagation and physical gradient update.** (a) Forward pass (nonlinear evolution) of the "evaluation" wave field Ψ in the presence of a background potential landscape provided by a "learning field" Θ . Any small perturbation $\delta\Theta$ will affect the output, as indicated here, which in turn changes the value of the cost function. (b) Instead of testing the cost function response for many potential updates of the learning field Θ , Hamiltonian Echo Backpropagation automatically produces the required update in a single backward pass, via physical dynamics. After applying a time-reversal operation ($\Psi \mapsto \Psi^*$), the subsequent nonlinear wave field evolution is a time-reversed version of the forward pass. A small variation $\delta\Psi$ injected on top can now be used to backpropagate the error signal (variation of the cost function at the output); see main text. This then leads to the required update of the learning field θ , via the physical interaction between Ψ and θ , realizing a fully autonomous learning machine.

single complex variable. We will reserve the capital greek letters for the complex variables, as follows: $\Psi = \psi + i\pi_\psi$, $\Theta = \theta + i\pi_\theta$, where the canonical coordinates and momenta have been rescaled to obtain the same dimension (nominally, square root of an action). This will make the notation for the time-reversal especially convenient, as it corresponds to a complex conjugation of the dynamical variables. Furthermore, one can easily check that Hamilton's equations can now be written in a particularly convenient manner:

$$\dot{\Psi} = -i\partial_{\Psi^*} H,$$

where one has to formally treat Ψ, Ψ^* as independent variables (or more technically, ∂_{Ψ^*} represents a Wirtinger partial derivative).

As a concrete example, let us assume that our cost function is simply the overlap between the target state and the output state. Then, the prescription above tells us we just have to inject a weak perturbation proportional to the target state: $\Psi(0) \rightarrow \Psi(0) - i\epsilon\omega\Psi_{target}$.

After this step, we time-reverse, which in our complex notation means to phase conjugate the fields, e.g. $\Psi \rightarrow \Psi^*$. In the limit $\epsilon \rightarrow 0$, Ψ will evolve backwards precisely to the input configuration, because the Hamiltonian is time-reversal-invariant. However, when ϵ is small

but finite, we obtain a small variation in the fields, both in Ψ and Θ . One can understand such variation as a perturbation traveling on top of the time-reversed field, from output to input. Once the back-propagation is complete, one obtains a slightly perturbed echo of both Ψ and Θ , at $t = T$. Since we have perturbed the field at $t = 0$, the echo is not perfect: there is a small variation given by $\Theta(T) = \Theta^*(-T) + \delta\Theta(T)$. In order to have the correct sign for the momentum of the learning field required for our approach, we time reverse again, $\Theta(T) \rightarrow \Theta^*(T)$. Using the self-reciprocity principle, one can then show that the final configuration of Θ in the echo step is simply given by

$$\Theta(T) = \theta(-T) - i\epsilon \frac{\partial C}{\partial \Theta^*(-T)}. \quad (5)$$

We will show below how to prove that result, which encapsulates the central idea of our proposal, mathematically (Sec. IV).

We note that the procedure introduced here differs in an important way from previous approaches to self-learning dynamics [4], which never considered a full time-reversal of the nonlinear wave field and instead treated a weak perturbation traveling against a strong forward-propagating field. It is a consequence of this choice that these approaches work only for some specific carefully chosen wave dynamics, and not in the general, Hamiltonian-independent way that we outline here.

The final step of HEB will be the update of the learning field, to be discussed now.

E. Implementing the physical learning field update

At this step, the dynamics of the learning field Θ almost looks like gradient descent, but not completely: we have been able to impart a momentum kick to Θ that is proportional to the gradient of the cost function, but what we really want is to update the position θ . We now need to convert the update in the canonical momentum into a shift in the position. For this purpose, we need a dissipative step. This is not surprising, because we have only used Hamiltonian evolution and time reversals so far, while the overall gradient descent procedure is contractive.

For simplicity, we will explain this step by means of an example that contains all the key ingredients needed. In this example, we assume that the effect of dissipation may be modelled by a damping force of the form $-\Gamma(t)\pi_\theta$, where $\Gamma(t)$ can be controlled in a time-dependent fashion. Furthermore, we assume that the dynamics of Θ in the absence of interaction corresponds to a free-particle Hamiltonian, $H_\theta = \Omega\pi_\theta^2/2$ (Note that in our convention π_θ^2 has units of action, which implies that Ω has units of frequency). The stable manifold would be given by the particle at rest at any location, with $\pi_\theta = 0$. This is, however, only one example out of all the systems that

can be trained with HEB; in the next subsection we will consider the most general case.

During this final step of the HEB procedure, we switch on the dissipation, $\dot{\pi}_\theta = -\Gamma\pi_\theta$, and apart from that we let Θ evolve freely. If we wait long enough, the final configuration of Θ is given by $\theta(-T) + \epsilon \frac{\partial C}{\partial \pi_\theta(-T)} - \epsilon \frac{\Omega}{\Gamma} \frac{\partial C}{\partial \theta(-T)}$ (to first order in ϵ), while the canonical momentum decays to zero. The update step finishes in the end of the decay step, at time $T_f \gg \Gamma^{-1}$. In the limit of large decay times, i.e. $\frac{\Omega}{\Gamma} \gg \frac{\partial C}{\partial \pi_\theta(-T)} \left(\frac{\partial C}{\partial \theta(-T)} \right)^{-1}$, we recover the usual gradient descent update rule

$$\theta(T_f) = \theta(-T) - \eta \frac{\partial C}{\partial \theta(-T)}, \quad (6)$$

with a learning rate given by $\eta = \epsilon \frac{\Omega}{\Gamma}$. Repeating this procedure in a sequential way, for many injected training samples, will realize stochastic gradient descent (SGD). Apparently, the learning rate is proportional to ϵ , which represents the duration during which the "cost function Hamiltonian" is active.

We must remark that in the general case, when H_θ is not necessarily a free-particle Hamiltonian, the relation of η to ϵ may be different. However, we can always expect these two quantities to be proportional, due to the assumption of injecting only a weak perturbation.

F. Summarizing the general scheme of Hamiltonian Echo Backpropagation

We are now in a position to summarize the general approach (Fig. 4). Let us assume that H_{int} is an arbitrary time-reversible Hamiltonian, and H_θ is some Hamiltonian with a degenerate ground state. Let us suppose further that Θ starts in one of the ground states of H_θ . The HEB procedure consists of a sequence of multiple events (Fig. 4a), but they can be subdivided into two big steps:

1. **Echo step.** We randomly draw an input sample from the training data set, and we use it to initialize $\Psi(-T)$. Following the nonlinear dynamics of the interacting system, the output is obtained at $t = 0$. At that point, the evaluation field is weakly perturbed according to $\Psi(0) \rightarrow \Psi(0) - i\epsilon \partial_{\Psi^*(0)} C$, which can be brought about via the dynamics induced by an extra interaction Hamiltonian (the "cost function Hamiltonian"), as explained above. Immediately afterwards, both Ψ and also the learning field Θ are time-reversed (i.e. phase-conjugated). At $t = T$, a perturbed echo of the initial configuration will be obtained. We then time-reverse Θ again at $t = T$. The final result of this whole process is equivalent to the following update of the learning field:

$$\Theta(T) = \Theta(-T) - i\epsilon \partial_{\Theta^*(-T)} C. \quad (7)$$

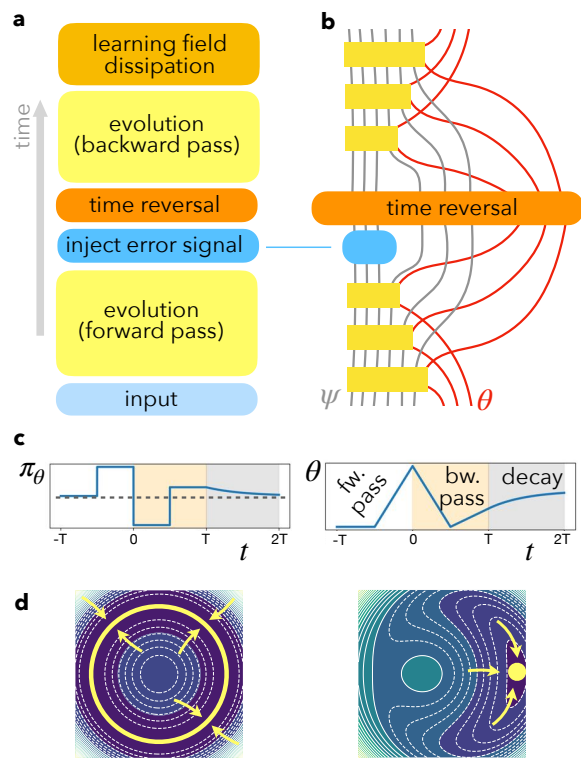


Figure 4. **Ingredients of a self-learning machine based on Hamiltonian Echo Backpropagation.** (a) Sequence of events. (b) Use of 'pseudo-dissipation' via ancillary modes. The learning field Ψ is here decomposed into a number of discrete modes. As time progresses, more and more modes do not participate any longer in the physical interaction (yellow boxes), becoming ancillary modes. Both these ancillary modes and the learning field θ also take part in time-reversal, however. (c) Time-evolution of the learning field momentum (left) and the field itself (right) during one forward-backward pass, including the effects of time-reversal (we show a single value of the field at one location). The momentum decays back to zero, but the field has been updated suitably. (d) The intrinsic dynamics of the learning field has a continuously degenerate ground state (i.e. a manifold attractor). Right: The effect of the training dynamics is to break this degeneracy and produce a minimum determined by the cost function.

To be clear, C here always is the sample-specific cost function. We show in detail how to prove this result in general in the next section. It has a simple interpretation: to first order in ϵ , the evolution of Θ satisfies Hamilton's equations, with an effective Hamiltonian equal to the cost function.

2. **Dissipative step.** The dissipation is switched on for a time interval T_D , and there is no interaction with Ψ (because $\Psi = 0$ during this step). The evolution of Θ is given by H_θ together with the dissipative effect of the coupling to the thermal bath. This will ensure the suitable update of the Θ field needed to implement SGD via the physical procedure explained here. Finally, proceed with the next

training sample.

The evolution of the learning field during the whole procedure is schematically depicted in Fig. 4c. Imagine that these two steps are alternated many times, with suitable small values for ϵ and T_D . Then the average dynamics of Θ is approximately described by an effective Hamiltonian given by

$$H_{\text{eff}} = \frac{1}{\epsilon + T_D} (\epsilon C + T_D H_\theta + T_D H_{\text{bath}}), \quad (8)$$

where C here represents the sample-averaged cost function. Remember that, in the absence of interaction with Ψ , the phase space of Θ has a stable manifold. Consider what happens in the low-temperature limit of the thermal dissipative reservoir that is used to act on Θ . When we set $\epsilon > 0$, we break the degeneracy of H_θ (see Fig. 4d). The dynamical process we described will tend to equilibrate the temperatures of Θ and the reservoir, so that Θ will tend to minimize the cost function, constrained to the manifold of ground states of H_θ . Once the training has converged, we can stop performing perturbed time reversals (in terms of the effective Hamiltonian, that is equivalent to setting $\epsilon = 0$). Since we have converged to one of the many degenerate ground states of H_θ , we are still in a stable point. In consequence, if the temperature of the reservoir is low enough, Θ will remain near the learned configuration for arbitrarily long times. That is of course important to ensure that, after training is completed, the SL machine doesn't quickly forget the result of the learning process. This line of reasoning does not depend on the particularities of H_θ , as long as it possesses some manifold of degenerate ground states.

This concludes our overview. The steps of the approach are illustrated in Fig. 5 in terms of a very simple mechanical Hamiltonian system, highlighting the generality of the procedure.

We now present a few additional considerations.

At first sight, one may argue that assuming the continuous degeneracy of H_θ is already a strong restriction on the possible physical implementations of Hamiltonian self-learning machines. In fact, if one can perform perfect time reversal operations outside the device, this assumption can also be dropped. Consider, for example, a device where both the evaluation and learning variables are given by wave fields that are sent through the device. In this way, the learning field is given by a superposition of wave packets that enter the device, interact with the evaluation field, and finally come out of the device at the end of the forward step. In this case, the time reversal operation (for both learning and evaluation fields) is performed outside the device. The learning field (as well as the evaluation field) then propagates backwards, realizing the echo step. At the end of the echo step, it comes out at the original input, where it has to be time-reversed again, also outside the device. The decay step would also be performed externally. The decay step would include

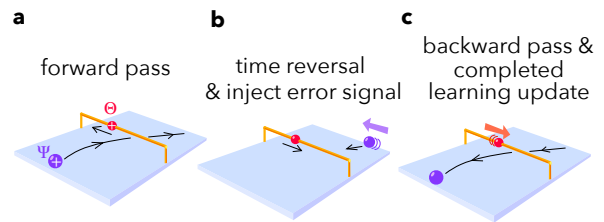


Figure 5. **Hamiltonian Echo Backpropagation in a simple mechanical model.** (a) A charged ball Ψ is launched with a velocity representing the input to the machine. Its trajectory is deflected depending on the position of another charged ball Θ , which can freely move along a rail and which experiences a momentum kick due to this interaction. (b) Eventually, the velocities of both balls are reversed, and the ball Ψ is slightly adjusted according to its deviation from the desired outcome ("error signal"). (c) Afterwards, it retraces almost exactly its initial trajectory, delivering yet another momentum kick to the Θ particle. Finally, any remaining velocity of Θ is dissipated and converted into a finite displacement, representing the training update. Of course, the expressive power of this machine, containing only these two degrees of freedom, is very limited (i.e. it can only produce very rough approximations to most input-output relations). Nevertheless, it illustrates the generality of the procedure – e.g. an arbitrary (even unknown) static force field acting on the Ψ particle will not spoil the learning procedure.

controllable dissipation and potentially other simple operations on Θ . For example, an operation that simulates the effect of a free-ballistic Hamiltonian, together with a controllable damping term, would make possible to realize SGD exactly, as discussed in the subsection 6. Crucially, all the external operations during the decay step must be also independent of the Hamiltonian of the device and they have to be realized in an autonomous way by means of physical processes. If this process is repeated sequentially, we can realize HEB even when the Hamiltonian of the device is not degenerate in θ . This is because the time-reversal operation is able to remove the overall effect of the Hamiltonian of the device during a full echo step. Therefore, our training method can be used in a way that is truly independent of the Hamiltonian of the physical device, with the only assumption that it is time-reversible.

Nevertheless, we considered in our analysis the presence of a degenerate term, H_θ , for two reasons. First, having a degenerate ground state manifold to which Θ can converge is helpful in order to improve the long term stability of Θ once it is trained: Unlike the most general case discussed in the preceding paragraph, this means we do not need to continue (external) time-reversal operations just to keep Θ stable.

Second, in many possible setups for a SL machine, it could be impossible to perform the time reversal operation and the decay step externally. When that is the case, the equations of motion during the echo step are given by $i\dot{\Theta} = \partial_{\Theta^*} (H_\theta + H_{\text{bath}})$. Then, the learning variables have

the freedom to minimize the cost function only when the term H_θ has a degenerate ground state.

Consider now what happens when the set of stable ground states of H_θ is in fact not continuous, but actually discrete. This may be the case if, for example, Θ describes a collection of degenerate parametric oscillators. In this situation, a gradient descent strategy would not succeed, as Θ cannot change continuously between fixed points. Nevertheless, our procedure for training can still minimize the cost function. Indeed, consider that we start from a relatively high temperature in the thermal reservoir. The thermal fluctuations in the reservoir would result in random jumps between the stable points. As our training procedure advances, we decrease the temperature of the reservoir, inducing annealing. In the end, if the system converges to a thermal equilibrium, the configuration of Θ would be found in one of the minima of the cost function.

In practice, controllable dissipation may be a too stringent requirement. Actually, we do not need to have control over the dissipation on Θ if the dissipation timescale is large enough. In order to see this, we require that the damping constant is weak enough that its effect can be neglected during one single evaluation step: i.e. the damping time-scale Γ^{-1} is much longer than the duration of the evaluation step T . The core of our procedure is to enact an effective force on θ that is proportional to the slope of the cost function. If the dynamics were purely conservative, that would not be sufficient, as Θ would oscillate around the stable manifold without ever converging anywhere. It is clear then that we need such a damping term. In consequence, we distinguish two time scales: the short time scale T of an evaluation step, in which all dynamics is approximately Hamiltonian and time-reversible, and the long time scale of the total training time, in which dissipation ensures that, in the end, Θ converges to the stable manifold.

G. Two variants of the self-learning machine architecture

A standard neural network architecture builds up the network out of layers, where information processing occurs sequentially. To avoid confusion, we emphasize right away that such a spatial arrangement and sequential processing are not at all needed for the general approach described here: all the degrees of freedom may be evolving in a nontrivial fashion all of the time. However, in some physical implementations it may be beneficial to choose such a layered structure anyway.

In practice, we can imagine two ways in which the SL machine is operated (Fig. 6). Perhaps the most straightforward way to realize HEB is that the time-reversal is effecteduated by a time-reversal device outside the machine. In this case, the input and output of the SL machine must be some traveling pulses of excitations. For example, it is possible to conceive a setup in which Ψ is an

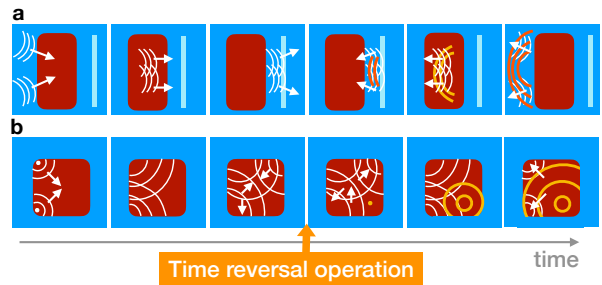


Figure 6. **Different architectures of a self-learning machine** (a) Time-reversal of the fields outside the device. In this setup, the input wave packets enter in the device, where they interact nonlinearly. As a result, an output wave field is produced, which continues to propagate until it is time-reversed by a phase-conjugating mirror (PCM). In addition, a perturbation is injected according to the target output (here indicated by additional waves). (b) Time-reversal inside the device. In this more general scenario, there is no clear direction of propagation. The time reversal operation cannot be realized by a PCM outside the device; instead all the fields have to be time-reversed simultaneously. Although we represent here continuous wave fields for simplicity, this could be more feasible experimentally in the case of a discrete lattice implementation, in which each node can be time-reversed at the same time.

optical pulse propagating in a given direction. The wave packet enters inside a photonic circuit (or a free-space setup), propagates inside, and finally exits at the output. Then, it arrives at a phase-conjugating mirror where it is time-reversed and sent back to the circuit (assuming a symmetric shape of the pulse in the propagation direction, or alternatively that the time-reversal is realized with an instantaneous time-mirror like in [20]). In principle, the Θ field could also be an optical pulse that is time-reversed in the same way.

However, in our derivation of the HEB, we will not need to assume such a specific implementation, with the Ψ field propagating through the device along a particular direction. In fact, there is a second - more general - possibility in which both Ψ and Θ are just fields interacting inside a device, with no predefined direction of propagation. This scenario requires the ability to instantaneously time-reverse the fields everywhere in the device at a particular time. We can imagine, for example, that both Ψ and Θ are optical fields inside an array of cavities. Using four-wave mixing it is possible to time-reverse all the cavities at the same time, thus realizing the backpropagating signal. Other physical platforms may offer different means of achieving the same goal, and we will discuss the time-reversal operation itself in subsection V C.

H. Invertible Dynamics vs. Contractive Maps

Before going any further, it is useful to introduce the concept of *pseudo-dissipation*. The goal of supervised

learning (both for classification and regression) is often to approximate a map from a set of high dimensional input vectors to a lower dimensional space. This is an inherently contractive process. Nevertheless, the fact that our theory of SL machines is based on reversible dynamics during the evaluation (forward pass) does not imply that it cannot be used for this purpose. It is always possible to embed contractive maps inside a higher-dimensional reversible map. In physical terms, we can introduce pseudo-dissipation: by introducing additional ancillary dynamical variables (which will also be considered part of Ψ in our formalism), we can simulate the effect of dissipation (Fig. 4b). We call it pseudo-dissipation because, unlike for real dissipation, we can still time-reverse the whole system, including the ancillary modes.

Pseudo-dissipation not only makes it possible to learn contractive maps, it is also useful to avoid chaotic dynamics. A practical SL machine must have a very complex dynamics, but it seems advisable to avoid the strong sensitivity on the input that is implied by chaotic dynamics. Pseudo-dissipation can prevent chaos in highly complex nonlinear systems, while preserving the feature of time-reversibility that is so important for our echo backpropagation approach.

To avoid confusion, we emphasize that this conceptual split of Ψ into the original evaluation field and additional ancillary degrees of freedom is irrelevant with respect to the following analysis of the echo step. Therefore, to simplify the notation we just consider the full vector Ψ without specifying how or whether it is split.

IV. ANALYSIS OF THE ECHO STEP

We now prove more formally that the crucial ingredient of our scheme, the echo step, indeed works as advertised above, deriving equation (7) in the most general setting.

In order to simplify the notation, we define $\Phi := \begin{pmatrix} \Psi \\ \Theta \end{pmatrix}$ as the joint configuration of all dynamical variables of the system. The dynamics of Φ is given by the following equation of motion

$$i\dot{\Phi} = \nabla_{\Phi^*} H, \quad (9)$$

where $H[\Phi]$ is the Hamiltonian. Crucially, we assume H to be time-reversal-invariant, which means $H[\Phi] = H[\Phi^*]$ in this notation. Let us remark here that time-reversal-invariance is the only assumption in this section (we do not need to assume a degenerate ground state for the expressions derived in this section). The operator ∇_{Φ^*} involves the derivatives $\partial/\partial\Phi_i^*$ and is formally defined as $(\nabla_{\Phi^*} f)_i = \partial f/\partial\Phi_i^*$. We stress that we will, at the moment, study the dynamics purely in the absence of coupling to the dissipative reservoir. In the notation of Eq. (1), $H[\Phi]$ corresponds to the first three terms of the SL Hamiltonian, $H = H_\psi + H_{\text{int}} + H_\theta$, without the bath.

A. Expression for the gradient of the cost function in terms of an 'advanced' backpropagating perturbation

In a SL machine, the output of an evaluation step is a function of the input $\Psi(-T)$ and the learning field, whose configuration at the initial time is given by $\Theta(-T)$. In the following, we want to obtain a formal expression for the gradient of C with respect to $\Theta(-T)$, which will later form the basis for physical backpropagation. Since Ψ and Θ are treated on an equal footing in Eq. (9), we will set out to find the gradient of C with respect to the initial value of the joint state $\Phi(-T)$:

$$\begin{pmatrix} \nabla_{\Phi^*(-T)} C \\ \nabla_{\Phi(-T)} C \end{pmatrix} = D \begin{pmatrix} \nabla_{\Phi^*(0)} C \\ \nabla_{\Phi(0)} C \end{pmatrix}, \quad (10)$$

where the matrix D is defined as

$$D := \begin{pmatrix} \nabla_{\Phi^*(-T)} \otimes \Phi^*(0) & \nabla_{\Phi^*(-T)} \otimes \Phi(0) \\ \nabla_{\Phi(-T)} \otimes \Phi^*(0) & \nabla_{\Phi(-T)} \otimes \Phi(0) \end{pmatrix} \quad (11)$$

and $[a \otimes b]_{ij} = a_i b_j$. Here the operator D obviously maps back changes in the output to corresponding changes in the input, and we will now relate it to the Green's function of the problem.

Suppose that $\Phi(t)$ is the solution of the nonlinear Hamiltonian equations when the initial conditions are given by $\Phi(-T)$. Let us consider what happens if we perturb $\Phi(-T)$ by some small $\delta\Phi(-T)$. This results in a weak perturbation $\delta\Phi(t)$ traveling forward on top of the zero-th order solution. One can write $\delta\Phi(t)$ as the solution to the linearized equations of motion:

$$L_\Phi(t) \begin{pmatrix} \delta\Phi(t) \\ \delta\Phi^*(t) \end{pmatrix} = \delta(t+T) \begin{pmatrix} -i\delta\Phi(-T) \\ i\delta\Phi^*(-T) \end{pmatrix}. \quad (12)$$

Here we introduced the linear differential operator

$$L_\Phi(t) = i \begin{pmatrix} +1 \\ -1 \end{pmatrix} \frac{d}{dt} - \begin{pmatrix} \nabla_\Phi \otimes \nabla_{\Phi^*} & \nabla_{\Phi^*} \otimes \nabla_{\Phi^*} \\ \nabla_\Phi \otimes \nabla_\Phi & \nabla_{\Phi^*} \otimes \nabla_\Phi \end{pmatrix} H[\Phi(t)]$$

in compact notation, with $[\nabla_\Phi \otimes \nabla_{\Phi^*}]_{ij} = \frac{\partial^2}{\partial\Phi_i \partial\Phi_j^*}$ and so on. If the vector Φ has M components, the operator $L_\Phi(t)$ acts on a space of dimension $2M$. The inhomogeneous term on the right-hand side of the preceding equation is there to enforce the initial conditions, assuming that $\delta\Phi = 0$ for $t \rightarrow -\infty$.

The solution of Eq. (12) can be written in terms of the retarded Green's function associated to $L_\Phi[t]$:

$$\begin{pmatrix} \delta\Phi(t) \\ \delta\Phi^*(t) \end{pmatrix} = \mathcal{G}_\Phi(t, -T) \begin{pmatrix} i\delta\Phi(-T) \\ -i\delta\Phi^*(-T) \end{pmatrix}. \quad (13)$$

The Green's function $\mathcal{G}_\Phi(t, -T)$ is a linear operator such that

$$L_\Phi(t') \mathcal{G}_\Phi(t', t) = \delta(t' - t) \mathbb{I}, \quad (14)$$

where \mathbb{I} is the identity matrix of size $2M$. Note that both L_Φ and $\mathcal{G}_\Phi(t, -T)$ depend on the zero-th order solution $\Phi(t)$ of the nonlinear dynamical equations, around which we have linearized. We chose $\mathcal{G}_\Phi(t, -T)$ to be the *retarded* Green's function, meaning that $\delta\Phi(t)$ originates at $t = -T$ and propagates in the forward direction of time. Causality dictates that $\mathcal{G}_\Phi(t', t) = 0$ for $t' < t$.

Employing the derivatives of the output $\Phi(0)$ with respect to the input $\Phi(-T)$, defined in Eq. (10), we see that

$$\mathcal{G}_\Phi(0, -T) = -D^\dagger i\sigma_z, \quad (15)$$

where σ_z is the Pauli matrix. Therefore, we have $D = -i\sigma_z \mathcal{G}_\Phi(0, -T)^\dagger$, and we can now express the change of the cost function in terms of the Green's function. However, we will see presently that it is helpful in terms of physical interpretation to introduce the *advanced* Green's function for this purpose, which also obeys Eq. (14) but has $\mathcal{G}^{\text{adv}}(t', t) = 0$ for $t' > t$ and represents a signal going backward in time. It is related to the retarded Green's function via

$$\mathcal{G}_\Phi^\dagger(t', t) = \mathcal{G}_\Phi^{\text{adv}}(t, t'). \quad (16)$$

Combining Eqs. (16), (15) and (10), we finally obtain a formula relating the gradient of C that is required for the learning update to the advanced Green's function and the (easily obtained) gradient of C with respect to the output fields:

$$\begin{pmatrix} \nabla_{\Phi^*(-T)} C \\ \nabla_{\Phi(-T)} C \end{pmatrix} = -i\sigma_z \mathcal{G}_\Phi^{\text{adv}}(-T, 0) \begin{pmatrix} \nabla_{\Phi^*(0)} C \\ \nabla_{\Phi(0)} C \end{pmatrix}. \quad (17)$$

This is still a formal expression at this point, but in the next section we will show how it can be implemented physically.

B. Time reversal of the perturbation: physical backpropagation

How can we produce the signal of Eq. 17 in practice, in order to allow the training update to take place? Apparently, we need to inject the source term $\nabla_{\Phi^*(0)} C$ as a perturbation and follow its "backwards time evolution".

Let us consider that, at $t = 0$, we have obtained the output Φ_{out} . Suppose that we have a way to implement an interaction Hamiltonian $C[\Phi]$ that is proportional to the cost function (written as a function of the output). Let us further suppose that we can control this interaction Hamiltonian, so that we can switch it on during some short period of time, and later switch it off again. In theory this is always possible, because a cost function is just a real function of the output. In practice, we will see that, depending on the cost function, this corresponds to driving the system, or applying phase shifts, or, for more

complicated cost functions, to realizing some nonlinear interactions. In any case, this operation is a function only of the output, not requiring any knowledge of or feedback on the internal degrees of freedom of the autonomous self-learning machine. As we will discuss later, a practical implementation is possible for several standard cost functions with relatively simple setups. For the moment, we consider the general case in which C is an arbitrary cost function. When we realize such an interaction Hamiltonian C , according to Hamilton's equations, the evolution will be given by $i\dot{\Phi} = \nabla_{\Phi^*} C$. Let us suppose that we only realize such interactions during an infinitesimally small time interval, ϵ . The result of such a brief Hamiltonian evolution is to update the fields as $\Phi(0) \mapsto \Phi(0) - i\epsilon \nabla_{\Phi^*} C$.

The advanced Green's function evolves a perturbation of the output backwards in time to obtain the corresponding perturbation of the input. In order to realize this physically, we need to induce the time-reversed evolution of the system. In a time-reversal invariant system (such as the one considered here), this is possible by implementing a time-reversal operation and then letting the natural dynamics proceed from there forwards in time. In the present complex notation, we know that a time reversal is equivalent to phase conjugation, $\Phi \mapsto \Phi^*$, flipping the momenta. By means of phase conjugation, applied to the already perturbed field, we produce a perturbed echo given by $\Phi^*(0) + i\epsilon \nabla_{\Phi} C \equiv \Phi_{\text{echo}}(0) + \delta\Phi_{\text{echo}}(0)$.

Importantly, the whole configuration of the system is time-reversed, and, as a consequence, the evolution for $t \in [0, T]$ is, to leading order, given by the fully time-reversed nonlinear evolution: $\Phi_{\text{echo}}(t) = \Phi^*(-t)$. The first order correction $\delta\Phi_{\text{echo}}(t)$ is the linear response of the system to the perturbation $i\epsilon \nabla_{\Phi} C$ in the initial conditions, evolving on top of $\Phi^*(-t)$.

Now we come to the crucial step. In any time-reversal invariant system, the advanced and retarded Green's functions of linear perturbations propagating on top of the original nonlinear dynamics and its time-reversed counterpart, respectively, are connected in the following way:

$$\mathcal{G}_\Phi^{\text{adv}}(t', t) = \mathcal{T} \mathcal{G}_{\Phi_{\text{echo}}}^{\text{ret}}(-t', -t) \mathcal{T}, \quad (18)$$

where $\mathcal{T} = \sigma_x$ is the time-reversal operation, interchanging $\delta\Phi$ and $\delta\Phi^*$. Therefore:

$$\mathcal{G}_\Phi^{\text{adv}}(-T, 0) \begin{pmatrix} \nabla_{\Phi^*(0)} C \\ \nabla_{\Phi(0)} C \end{pmatrix} = \mathcal{T} \mathcal{G}_{\Phi_{\text{echo}}}^{\text{ret}}(T, 0) \begin{pmatrix} \nabla_{\Phi(0)} C \\ \nabla_{\Phi^*(0)} C \end{pmatrix} \quad (19)$$

It is now obvious that the left-hand-side, which (as we have already found above) formally yields the update needed for the gradient descent, can be *physically* implemented in terms of the right-hand-side version, with a suitable perturbation injected and propagated *forward* in time on top of the echo. Finally, as we can see from Eq. (19), at $t = T$ we have to perform a final time-reversal (phase-conjugation) again.

Overall, after the whole process is completed, we obtain a replica of the initial configuration at $t = -T$, but importantly with a small correction that is proportional to ϵ . The result of the whole physical process can be summarized as

$$\begin{pmatrix} \Phi(T) \\ \Phi^*(T) \end{pmatrix} = \begin{pmatrix} \Phi(-T) \\ \Phi^*(-T) \end{pmatrix} + \mathcal{T} \mathcal{G}_{\Phi_{\text{echo}}}^{\text{ret}}(T, 0) \begin{pmatrix} \epsilon \nabla_{\Phi(0)} C \\ \epsilon \nabla_{\Phi^*(0)} C \end{pmatrix}. \quad (20)$$

We can convince ourselves that this is the learning update that was needed, by reformulating the deviation (second term on the right-hand-side) with the help of Eq. (19) and subsequently Eq. (17)]. This produces:

$$\begin{pmatrix} \Phi(T) - \Phi(-T) \\ \Phi^*(T) - \Phi^*(-T) \end{pmatrix} = -i\epsilon\sigma_z \begin{pmatrix} \nabla_{\Phi^*(-T)} C \\ \nabla_{\Phi(-T)} C \end{pmatrix} \quad (21)$$

This is exactly the learning update that was needed, according to Eq. (7), for the learning parameters Θ . Incidentally, the evaluation degrees of freedom Ψ have also changed, but they will be discarded when the next input is injected into the learning machine.

V. POTENTIAL INGREDIENTS OF PHYSICAL IMPLEMENTATIONS

The most important feature of our new method is its generality. It can be used to train any time-reversible Hamiltonian physical system. It is not our intention here to give a full description of all possible implementations of the SL machine. On this general level, we cannot even decide which ones are optimal, as the most suitable architecture is heavily dependent on the machine learning task of interest. Nevertheless, we can give some guidelines.

The main ingredients of any SL machine of the type presented here are: a time-reversal-invariant Hamiltonian system with two sets of dynamical variables Ψ and Θ ; a device or method to transform the output according to the cost function Hamiltonian (injecting the error signal), and a device that can time-reverse Ψ and Θ . There must be a physical distinction between Ψ and Θ , in that Θ needs to be multi-stable, i.e. it can remain indefinitely in one location of a higher-dimensional attractor, in the absence of its interaction with Ψ – turning it into the ‘learning field’. In theory we also need a way to control dissipation; in practice it may be enough to ensure that its effect is negligible during the echo step. In this section, we will discuss each of these ingredients on a general level, and we will provide a summary of some of the most promising possibilities for their realization.

A. Ingredients of the Hamiltonian: Linear and nonlinear parts

The dynamics of Ψ and Θ is given by the Hamiltonian H_{SL} . In Eq. (1) we split H_{SL} in four terms. The first two

terms, H_{Ψ} and H_{int} , are the ones that govern the evolution of Ψ and its interaction with the learning degrees of freedom. The second term, H_{Θ} , is concerned with the stabilization of the learning degrees of freedom. The only goal of H_{Θ} is to provide a degenerate ground state for Θ , so that the phase space of Θ has many different stable points to which it can converge during training. The fourth term, H_{bath} , accounts for the controllable time-dependent damping that is necessary for the dissipative step of HEB. The details of H_{bath} are not important. We only require that its effect can be made negligible during the echo step, and that it doesn’t break the degeneracy of \mathcal{H}_{Θ} .

Let us start with the discussion of H_{Ψ} and H_{int} . If one wants to use a SL machine for any useful task, the dynamics of Ψ must be complex and nonlinear. The expressive power of ANN’s can only be matched if the equations of motion for Ψ incorporate nonlinear interactions, as well as interactions with the learning parameters encoded in Θ . However, the input-output relation must be deterministic and robust to small amounts of noise. These considerations should guide the choice of the Hamiltonians.

As we discuss later in this section, there is a considerable amount of theoretical and experimental work about the time reversal of wave fields, especially in nonlinear optics. For this reason, here and henceforth we will concentrate on approaches based on nonlinear wave fields. Here, $\Psi(\mathbf{x})$ and $\Theta(\mathbf{x})$ are complex fields defined on a continuous space, or in a discrete lattice. Although we make extensive use of a notation that is reminiscent of optical fields, we must remember that, actually, the setting is completely general (the real and imaginary parts of the field are the two conjugate coordinates of a completely general Hamiltonian degree of freedom). However, the fact that we have now assumed $\Psi(\mathbf{x})$ and $\Theta(\mathbf{x})$ to be fields allows us to make use of the notion of locality.

In a SL machine based on wave fields, H_{Ψ} would be composed of two parts: a *free-field* Hamiltonian H_0 , and a second term H_{NL} containing local self-interactions. We can define a free-field Hamiltonian as any quadratic function of Ψ, Ψ^* and its time- and space-derivatives. More restrictively, we can ask that H_0 is invariant with respect to a global phase shift of Ψ , so that the total intensity, $\int d^D x |\Psi|^2$, is a conserved charge. In that case, H_0 can only contain second-order terms that are bilinear in Ψ, Ψ^* .

To produce non-linear dynamics, we introduce the self-interacting term, H_{NL} . Often, this will be a local term. Typical examples of self-interaction Hamiltonians would be the familiar Kerr nonlinearity, $g|\Psi|^4$, or a Josephson nonlinearity, $\chi \cos \psi$, that can become relevant for superconducting circuit quantum electrodynamics.

The free-field Hamiltonian together with a self-interaction is enough to obtain very complicated dynamics. But if we want to train the SL machine, we still need to introduce some dependence on the learning parameters through the interaction Hamiltonian, H_{int} . In analogy

with ANN's, we may ask that the interaction produces dynamics linear in Ψ , although this is not a requirement. Moreover, H_{int} will also be local in most realistic settings. Therefore, the most reasonable choices for H_{int} are $g\Theta^*\Theta\Psi^*\Psi$ (in nonlinear optics, this is called *cross-phase modulation*), or $g(\Theta + \Theta^*)\Psi^*\Psi$ (the standard $\chi^{(2)}$ interaction in optics, or equivalently an optomechanical interaction), or in general some interaction of the form $f(\Theta, \Theta^*)\Psi^*\Psi$. Alternatively, parametric interactions of the type $f(\Theta, \Theta^*)\Psi^*\Psi^* + \text{c.c.}$ could also be considered, leading to a different kind of dynamics, although we will not discuss them here.

The Hamiltonian terms we described could be homogeneous across space, like in the case of an optical field propagating inside a nonlinear crystal, or they could be implemented using discrete building blocks, as it would be the case for a photonic or microwave circuit with nonlinear elements. It can be argued that the evolution of Ψ under the joint action of $H_0 + H_{\text{int}} + H_{\text{NL}}$ is very similar to the evaluation of an ANN (as argued in other works before, see e.g. [4, 12, 21]). On the one hand, the effect of H_{NL} is to induce a nonlinear activation function. On the other hand, the part $H_0 + H_{\text{int}}$ is quadratic in Ψ and can be thought of as implementing the trainable matrix of weights.

It is known that local controllable shifts together with fixed unitary operations are enough to realize any unitary transformation [22]. Of course, it needs to be noted that standard ANNs can have arbitrary weight matrices between layers, which seem to go beyond the unitary matrices available in the present setting. However, any arbitrary matrix can be embedded in a larger unitary matrix (with proper rescaling). For this reason, the structure of the linear part of the ANN can always be replicated in a SL machine. Alternatively, we may view an SL machine with unitary evolution as realizing a particular case of an invertible neural network.

B. Pseudo-dissipation

As we said in an earlier section, pseudo-dissipation can be a useful feature in a SL machine. We can imagine that in our SL machine there are dynamical variables that are coupled to Ψ until some particular time, after which they evolve separately. Instead of explicitly switching off the couplings as a function of time, we might also just have wave fields propagating out of the region where interactions are present. This can easily be arranged, e.g. in photonic circuits. The ancillary dynamical variables carry away part of the information, reconciling the contractive mapping with the overall time-reversal symmetry of the SL machine. We start with a high dimensional input, but as time passes, the dimension of the interacting part of the system is increasingly reduced. In the end, the dimension of the output may be much smaller than the original input dimension. Importantly, in the echo step of HEB, the output and the ancilla must be

both time-reversed.

Pseudo-dissipation via ancillary modes can play an important role for the activation functions implemented via nonlinearities. As we already mentioned, the nonlinear evolution induced by the self-interaction Hamiltonian can be understood as an activation function. It is desirable to choose H_{NL} in such a way that the induced activation function is not oscillatory and has a bounded derivative. Ideally, a monotonic function would be the best option, reproducing standard ANN activation functions. In most previous approaches to physical learning with nonlinear optical devices, the nonlinearity is provided by a homogeneous Kerr self-interaction. The effect of a Kerr nonlinearity is to induce a phase shift proportional to the intensity of the field. Qualitatively, we can think of a Kerr medium as a deep neural network where the activation function is of the form $f(\Psi) = e^{ig|\Psi|^2}\Psi$. This is an oscillatory function, which is an undesirable property for an activation function in an ANN. What is worse, the derivative of the Kerr phase shift grows without bounds for increasing intensity. If we want to mimic the behaviour of a sigmoid or ReLU activation function, we must incorporate ancillary degrees of freedom, because all such standard activation functions are contractive. One possible choice is to use a $\chi^{(2)}$ nonlinearity, and to couple an ancillary mode to the evaluation field: $H_{\text{SI}} = \chi^{(2)}(\Psi_{\text{anc}}^*\Psi^2 + \Psi_{\text{anc}}\Psi^{*2})$. When the ancillary field is initially $\Psi_{\text{anc}} = 0$, the absolute value of $\Psi(t)$ as a function of the absolute value of the input is qualitatively similar to a sigmoid function (although it is not a monotonic function):

$$\Psi(t) = \Psi(0)\text{sech}\left(2^{-1/2}\chi t|\Psi(0)|\right). \quad (22)$$

Aside from $\chi^{(2)}$ nonlinearities, it is certainly also possible to produce an adequate activation function by a judicious combination of ancillary modes and a Kerr self-interaction Hamiltonian, or other kinds of self-interaction. Sigmoid-like thresholders based on optical Kerr effect have been previously described[23], as well as bistable optical switches [24]. It is known that the Kerr interaction in combination with linear operations can be used to construct the Fredkin gate, and therefore it is universal for classical reversible computation [25].

C. Time reversal

For any time-reversible Hamiltonian, the evolution can be reversed by inverting the momenta: $\pi \rightarrow -\pi$. In our complex notation, that means to perform a phase conjugation of the fields: $\Phi \rightarrow \Phi^*$. Importantly, this step cannot be realized with purely Hamiltonian evolution, not even by breaking time-reversal symmetry momentarily. A time-reversal operation does not preserve the Poisson brackets, so it is not a canonical transformation. However, one can circumvent this problem by using ancillary modes. Let us consider that we have a dynamical variable

Φ that we want to phase-conjugate. Additionally, we also have a second, ancillary dynamical variable Ξ . An important assumption is that the initial value of the ancilla is $\Xi_{\text{in}} = 0$. The phase conjugation can then be realized in three steps. First, we couple Φ and Ξ in such a way that, after a fixed time, we have that $\Xi = \Phi_{\text{in}}^*$. This step can be realized with Hamiltonian dynamics. For example, a Hamiltonian of the "parametric interaction" form $H = \chi(\Phi\Xi + \Phi^*\Xi^*)$ would result in the desired outcome after an interaction time $t = \chi^{-1} \log(1 + \sqrt{2})$. Second, we swap both modes, so that $\Phi = \Phi_{\text{in}}^*$. This step can also be the result of Hamiltonian evolution, now choosing $H = \chi(\Phi\Xi^* + \Phi^*\Xi)$. Third, we erase the state of the ancilla, so that $\Xi = 0$ again.

Time-reversal has been experimentally realized in several platforms. In nonlinear optics [26], phase-conjugating mirrors are routinely implemented by means of three- and four-wave mixing processes [27]. In a theoretical paper by Miller [20] it was shown that four-wave mixing can be used to time-reverse optical pulses. This can be extended to any platform where four-wave mixing is possible, from microwave circuits [28] to cold-atom clouds [29].

D. Stabilization of the learning field

Once training via HEB has been completed and the cost function has been minimized, the learning parameters should remain stable for long times. The problem then is how to choose a physical system with degrees of freedom that can remain stable in a continuum of states. Mechanical degrees of freedom would be a priori a good selection. The position of freely moving nanoparticles or the orientation of a (possibly levitated) rotor (e.g. a molecule or nanorod) are examples of systems that could store a degree of freedom for indefinitely long times. The problem is that the time-reversal of mechanical systems has no straightforward solution. The possible exception to this statement are optomechanical systems, where the coupling to the light field can be employed to time-reverse mechanical motion, but then the mechanical degree of freedom oscillates around a single equilibrium position, making it unsuitable for our purposes absent any additional ingredients. By contrast, in the case of wave fields, the experimental techniques for phase conjugation are better known, but storing information for longer times is more problematic.

The solution is to engineer a suitable physical system that has the desired characteristics. Modern systems in integrated nonlinear optics and in superconducting microwave circuits allow for the design of a wide range of nonlinear interactions between localized modes of the radiation field. In the following, we provide two examples of how this flexibility might be exploited to design a degenerate ground state manifold for a learning field.

In the first example, we consider a cavity that has two modes α_1, α_2 with the same frequency (like coun-

terpropagating modes in a microresonator). Inside the cavity there is a nonlinear material that induces a repulsive Kerr-type interaction. Both modes have the same lifetime. In order to have stable states with non-zero amplitude, we couple both modes to a parametric drive. Let us define the quadratures of the field modes as $q_{1,2} = \text{Re}\{\alpha_{1,2}\}/\sqrt{2}$, $p_{1,2} = \text{Im}\{\alpha_{1,2}\}/\sqrt{2}$ and introduce the abbreviations $Q^2 := q_1^2 + q_2^2$, $P^2 := p_1^2 + p_2^2$. In terms of the quadratures, the full Hamiltonian reads

$$H = -\chi\beta Q^2 + gQ^4 + (\chi\beta + 2gQ^2)P^2 + gP^4. \quad (23)$$

This Hamiltonian is written in the frame rotating at the mode frequency, and we assumed the parametric drive amplitude β is purely real-valued. It is not hard to see that this Hamiltonian is qualitatively similar to that of a point particle moving inside a 'Mexican hat' potential. Using this analogy, it is clear that any state with $P = 0$ and $Q^2 = \chi\beta/(2g)$ is a ground state. We could consider the angle in the (q_1, q_2) -plane as our learning parameter θ . In order to couple to this parameter, the simplest option we found is to suppose that Ψ interacts differently with α_1 and α_2 . For example, let us consider that there is a nonlinear element that couples Ψ only to α_1 , through a cross-phase modulation. The interaction Hamiltonian then can be written in terms of the learning parameter as $H_{\text{int}} = g \cos^2 \theta \Psi^* \Psi$.

Of course, storing a learning parameter in the amplitudes of parametrically driven Kerr oscillators is not the only possibility. As a further example, we briefly present another setup in which θ is the relative phase between two modes. Consider two modes α_1, α_2 that are also parametrically driven. The two modes α_1, α_2 have different frequencies given by ω_1, ω_2 , respectively. This physical system can be modelled by a Hamiltonian given by $\chi^{(2)}(\beta\alpha_1^*\alpha_2 + \beta^*\alpha_1\alpha_2^*) + \sum_{j=1}^2 \omega_j \alpha_j^* \alpha_j$. It is clear that this Hamiltonian is invariant with respect to any global phase shift $\alpha_j \rightarrow e^{i\varphi} \alpha_j$, $j = 1, 2$. Let us introduce the notation $\alpha_j \equiv |\alpha_j| e^{i\varphi_j}$, where φ_1, φ_2 are the phases of α_1, α_2 , respectively. We define the learning parameter as $\theta := \varphi_1 + \varphi_2$. Because of the symmetry of the Hamiltonian, θ is a free parameter in the ground state. The challenge is now to find a way to couple Ψ to the learning parameters. One possible way is to consider that Ψ has two components (field modes) Ψ_1, Ψ_2 . Choosing adequately the frequency of the modes Ψ_1, Ψ_2 , the product $g\alpha_1\alpha_2\Psi_1^*\Psi_2 + c.c.$ can be made resonant. Then, θ parametrizes a linear interaction between the two components of Ψ . This requires frequency stabilization of the difference frequency of Ψ_1 and Ψ_2 vs. the sum frequency of α_1 and α_2 . The advantage, though, is that now the symmetry of the Hamiltonian is more robust.

As we illustrated above, in order to engineer a physical system that can store a continuous learning parameter, we need to realize a Hamiltonian with some continuous symmetry. The problem is that in any real implementation we may expect that any continuous symmetry will be broken at some energy scale. If that is the case, most configurations of the learning field after training will have

a finite lifetime. Remember that we assume that, after training, the learning field ends in one of the degenerate ground states of H_θ , which is an ideal, exactly degenerate Hamiltonian. If the true Hamiltonian of the system is instead given by $H_\theta + H'$, the learning field will slide down in the energy landscape of H' . Eventually, it will end up very far from the configuration that had been obtained as a result of training, unless the training is periodically repeated to stabilize the "memory" of the system.

That potential problem could be avoided if the learning parameters were stored in a discrete set of states. Consider that now H_θ possesses a discrete set of degenerate ground states. In such a case, a small perturbation in H_θ does not affect the long term stability of θ , as long as it is much smaller than the energy barrier between the degenerate states. Stochastic gradient descent (SGD) is a strategy used to optimize continuous degrees of freedom. Although HEB is originally motivated by the search of a physical realization of SGD, we already argued that it can still be useful for training discrete parameters. In that case, HEB works in an analogous fashion to thermal annealing. In this picture, one can think of θ as a spin system that can be approximately described by a thermal distribution. The probability of each state is then given by $e^{-\beta H_{\text{eff}}[\Theta]}$, where $H_{\text{eff}}[\Theta]$ is the effective Hamiltonian of Eq. (8). If the temperature is slowly reduced, the system will undergo annealing, and Θ would end in one of the local minima of $H_{\text{eff}}[\Theta]$. Spin-like degrees of freedom can be realized, for example, with Optical Parametric Oscillators [30].

E. The cost function Hamiltonian

The cost function is another essential ingredient in the design of a SL machine. In our prescription for HEB, one crucial step is to inject the learning signal by perturbing the output fields according to $\Psi(0) - i\epsilon \nabla_{\Phi^*} C$, where C is a Hamiltonian that is proportional to the cost function. For arbitrary cost functions, this could always be achieved via some external processing and feedback, but as a general rule of course we want to avoid such steps. However, for simple cost functions, it could be possible to engineer a physical system whose evolution is actually described by the cost function Hamiltonian C .

In the case of the Mean Square Error (MSE) cost function, a physical implementation is relatively easy. The MSE cost function is defined as the squared difference between the actual output and the target output:

$$C[\Psi(0)] = \int dx g(x) |\Psi(0) - \Psi_{\text{target}}|^2. \quad (24)$$

Here $g(x)$ is position-dependent and will be zero in the areas that correspond to the ancillary degrees of freedom (which will be time-reversed, but not compared against any target). Expanding the square, we can write the corresponding Hamiltonian as $C[\Psi(0)] = g(x) |\Psi(0)|^2 - 2g(x) \text{Re} \{ \Psi(0) \Psi_{\text{target}}^* \}$ (where we have

dropped $|\Psi_{\text{target}}|^2$, which is just an irrelevant constant term). In terms of a physical wave field, the first term, $g |\Psi(0)|^2$, is just a shift in the frequency of the field. Its effect on $\Psi(0)$ is to induce a phase shift given by $e^{-i\epsilon g(x)}$. The second term, $-2g \text{Re} \{ \Psi(0) \Psi_{\text{target}}^* \}$, is nothing but a drive proportional to the target. In other words, this term can be realized straightforwardly by injecting a weak copy of the target field distribution, adding it to the wave field Ψ .

Alternatively, the MSE cost function can be also realized using the intensity of the field. Now, instead of forcing $\Psi(0)$ to match a target field, we only try to match a target intensity distribution. In that case, the cost function Hamiltonian is given by $C[\Psi(0)] = g |\Psi(0)|^4 - 2g |\Psi(0)|^2 I_{\text{target}}$. The experimental realization of $C[\Psi(0)]$ is reduced to a homogeneous Kerr non-linearity combined with a phase mask proportional to the target intensity pattern.

Other cost functions may be realized with different interactions. Which one is optimal would depend on the problem at hand and how the output is encoded in the physical fields. In many cases, the choice of the cost function would not be a critical feature.

VI. ILLUSTRATION IN NUMERICAL EXPERIMENTS

In this section we illustrate Hamiltonian Echo Backpropagation in two specific examples, by means of numerical simulations. Both examples rely on nonlinear wave propagation, of the kind that might be implemented in photonic neural networks. In the first case, we consider a self-learning machine with a very simple setup and we train to learn a logical function. In the second example, we consider a more elaborate architecture inspired by convolutional neural networks. We train the self-learning machine to perform classification on the standard MNIST handwritten digits data set. We believe that a more sophisticated architecture or other choices of the activation function and the cost function could improve the results even further, beyond the validation accuracy of 97.5% observed here. However, our primary goal here is to illustrate the concept, rather than constructing the optimal setup. In both scenarios, we simulated the full Hamiltonian Echo Backpropagation procedure, involving both the forward and the backward pass.

The setup considered in the first example consists of a nonlinear wave field. The dynamics of the evaluation field Ψ is given by the nonlinear Schrödinger equation coupled to the learning field

$$i\dot{\Psi} = \frac{\beta}{2} \nabla^2 \Psi + (\chi\theta + g|\Psi|^2) \Psi. \quad (25)$$

The learning field Θ permeates the nonlinear medium and it interacts with the evaluation field through an interaction of the optomechanical (or $\chi^{(2)}$) type. The evaluation field is initially prepared in a superposition of wave-

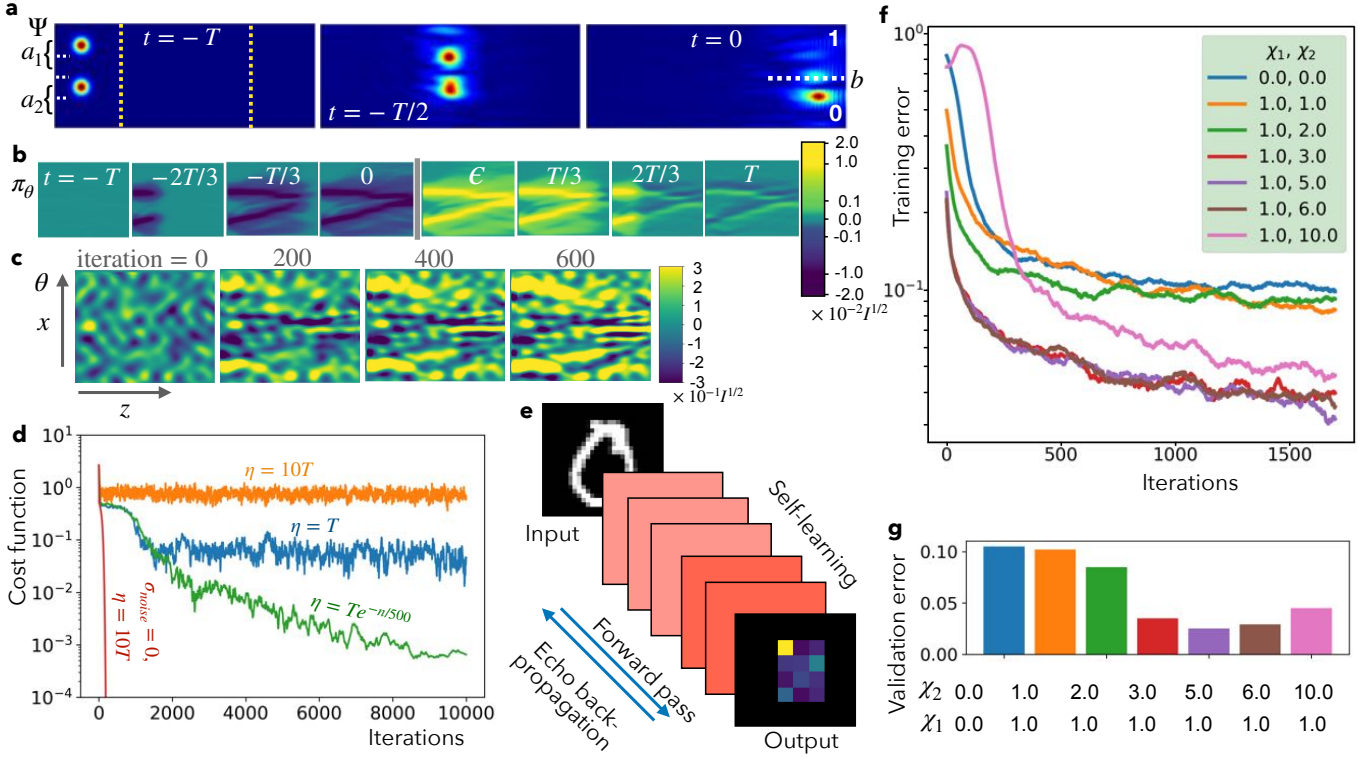


Figure 7. **Training a self-learning machine (simulations).** (a) Time-evolution of the "evaluation field" intensity $|\Psi|^2$ during a forward pass for a machine that has learned to implement XOR ($b = a_1 \oplus a_2$). The region in which the interaction with the learning field occurs is enclosed by yellow dashed lines. (b) Time evolution of the learning field momentum π_θ during a single training step. The pattern builds up from left to right as the Ψ pulse propagates. It is time reversed and then partially deleted as the Ψ pulse travels back. The finite remainder at time T is due to the injected error signal and produces the desired learning update. (c) Evolution of the learning field θ during many training steps. The training started with a smooth random configuration, and there are 600 HEB steps (each for a different randomly chosen training sample). (d) Analyzing the influence of a noisy time-reversal operation on training. Cost function during training for different values of the learning rate, at a fixed finite noise level whose standard deviation is given by $\sigma_{noise}^2 = 0.05I$ (see Appendix A for details). (e) Setup of a self-learning machine that learns to classify handwritten digits (MNIST). The outcome is a one-hot encoding of the detected digit, i.e. one of 10 patches "lights up". (f) Training error evolution of the MNIST setup for different strengths of the wave field nonlinearity. χ_1 and χ_2 are the nonlinear strengths at the convolutional and dense layers, respectively. (g) Final validation set classification accuracy.

packets that encode the input (Fig. 7), with initial momentum $k_z > 0$. Thus, they propagate from left to right, accumulating the effect of the nonlinear self-interaction and the interaction with the learning field. The output intensity is measured at two points, $\mathbf{x}_0^{out}, \mathbf{x}_1^{out}$. The output is considered a logical 0 if $|\Psi(\mathbf{x}_0^{out}, 0)| > |\Psi(\mathbf{x}_1^{out}, 0)|$; otherwise, it is a logical 1 (for more details, see Appendix A). The goal is to learn the exclusive-or (XOR) function mapping from input to output. As can be seen in Fig. 7, this is achieved rapidly.

The operation of a SL machine is independent of the Hamiltonian, and therefore one does not even need to know the particularities of the device (including any possible deviations from intended fabrication) to make it work. This is true because the time-reversal operation produces an exact inversion of the Hamiltonian evolution, for any time-reversible Hamiltonian. One could then wonder how sensitive HEB becomes to the preci-

sion of the time reversal. In fact, since the nonlinear processes used to phase-conjugate signals can also amplify noise, there are practical limits to the performance of a time-reversal mirror. Nevertheless, we will show here that the effects of noise in the time-reversal can be mitigated, although at the price of a longer training time. In 7(b), we compare the results using a perfect time-reversal (red line) with the results obtained in the case of a noisy phase conjugation, for several values of the learning rate (orange and blue), as well as for a suitably chosen time-dependent learning rate ("learning rate schedule", an approach also known for ANNs, with n denoting the training step index). As it could be expected, the performance of the SL machine deteriorates when the time-reversal is noisy. However, one can observe that decreasing the learning rate improves the final accuracy. This is because the overall update after several steps will approximately cancel out the random

noise, if the learning rate is small enough. Indeed, the backpropagating perturbation is a linear function of the error signal, to first order in ϵ . Therefore, the update of Θ in each step will be the sum of the appropriate gradient update plus a random signal that is proportional to the noise in the time-reversal. If each update step does not change the value of Θ significantly, the overall change after several steps will average out the unwanted noise. Note that this behaviour only applies to temporally fluctuating noise. In case of static systematic deviations from the correct time-reversal operation, an independent calibration of that operation would be required. Importantly, however, that would not rely on any knowledge of the internal dynamics of the SL machine.

The setup that we consider for the second example is inspired by the photonic neural network introduced theoretically by Ong et al [31]. It is composed of three convolutional layers followed by a dense fully-connected layer. The nonlinearity is provided by a $\chi^{(2)}$ optical nonlinearity, as described in Eq. (22). The convolutional layers can be implemented by a combination of Discrete Fourier Transforms (DFTs) and learnable phase shifts. The proposal by Ong et al. did not address the problem of how to implement the dense layers; we introduce an implementation of the dense layers that is based on a sequence of DFTs, learnable phase shifts and a linear interaction with ancillary degrees of freedom (see Appendix B). As a cost function, we choose the mean square error on the intensity.

In this setup, the learning parameters are all in the form of phase shifts. We assume that these phase shifts are produced by an interaction of the type $H_{int} = \theta\Psi^*\Psi$ inside some optical cavities through which the evaluation wave field travels.

In our simulations, the best results were obtained by choosing values of the nonlinear coupling strength that are different in the convolutional and the dense layers. This can be explained by the fact that the intensity decays as the wave packets propagate, as a result of the interaction with the ancilla modes. Therefore, it is optimal to choose that the nonlinearity in the dense layer, χ_2 , is stronger than the nonlinearity in the convolutional layers, χ_1 . The results in figure 7 show the training progress for several values of χ_1 and χ_2 . First we show the linear case, when $\chi_1 = \chi_2 = 0$, and then we sweep across several values of χ_2 , with fixed χ_1 . One can see a sharp transition in the achievable accuracy when χ_2 is increased. When the nonlinearity surpasses some threshold ($\chi_2 \approx 3$), the accuracy jumps from around 90% to above 95% (Fig.7g). This result suggests that at this point the device becomes a universal approximator. Our observations are in qualitative agreement with the findings by Marcucci et al. [32], where the expressive power of information processing using nonlinear wave fields was analyzed.

VII. POTENTIAL HARDWARE PLATFORMS

The elements for a SL machine that we have presented so far can be realized in many platforms. In fact, many of the ingredients needed for implementations of our proposal have already been demonstrated experimentally. In some cases, the physical platforms that we consider below were even already studied in the specific context of building new ML hardware, but it was not known how to train them successfully with physical procedures, without the use of external computation and feedback. Hamiltonian Echo Backpropagation can now provide a means to do this. Our only aim here is to give a brief overview of the possibilities. It is clear that for each platform substantial further research will be required to come up with an optimized design respecting the particular hardware constraints, and to analyze the potential performance as well as to take steps towards first experimental realizations.

In the nonlinear optics approach to neuromorphic computing, on-chip photonic circuits are one of the most discussed technologies for ML hardware. In a photonic circuit, Ψ is an optical field propagating inside an array of waveguides, and Θ may be stored in a series of optical cavities. We have pointed out above how suitable parametric driving can stabilize the learning field in a degenerate manifold. However, photonic circuits are not the only possibility in the realm of nonlinear optics: in the spirit of [4], Ψ and Θ could be optical pulses of light propagating inside a homogeneous nonlinear crystal. In principle, the storage of Θ could be achieved by recording its configuration in a hologram [4, 5], which at the same time also provides the means for its phase conjugation. While the ingredients are therefore known, additional research is undoubtedly needed on how to apply HEB in this kind of platform.

Microwave circuits are yet another promising platform for the implementation of a SL machine. The necessary nonlinearity can be provided by superconducting elements [33]. The advantage of superconducting microwave circuits is that these nonlinearities can be made arbitrarily strong and present experiments have reached an exceedingly high level of control, thanks to the drive towards quantum computation and simulation. Of course, such devices are inherently less compact than those in optics.

Approaches not based on electromagnetic fields are also possible. Clouds of cold atoms or molecules, possibly trapped in optical lattices, offer the possibility of storing information in the density distribution or the molecular orientation, making longer-term storage of the learning field Θ in principle less challenging than in the case of optical cavities. The interaction of an optical field Ψ with the atomic or molecular cloud would also provide strong nonlinear self-interactions. Alternatively, Ψ itself could be a (macroscopically populated, classical) matter wave, interacting with the cloud.

Likewise, spin waves share all the required ingredients

for a SL machine. We must remark that time-reversal symmetry must not be broken, which means that spin-spin interactions may be acceptable, but not (for example) light-magnon interactions via the Faraday effect. In the case of spin waves, there are already experimental demonstrations of strong nonlinear interactions that give rise to sigmoid-like activation functions [34].

Physical fields in real space are not the only possibility. So-called Ising machines have received a lot of attention in recent years [30, 35]. An Ising machine is a time-multiplexed train of pulses inside a fiber loop with a degenerate optical parametric oscillator (OPO). Due to the interaction with the OPO, the pulses have two degenerate stable states that can be treated as spin-like variables. A linear device in the fiber loop couples the pulses in a way that is reminiscent of an Ising Hamiltonian. In this way, an artificial lattice can be implemented with just a single fiber loop. This setup has all the elements needed for our proposal: it has very complex nonlinear dynamics, it is possible to engineer a degenerate ground state for Θ , and it can be time-reversed. As opposed to a standard photonic circuit, it is only necessary to realize a single nonlinear element, the OPO.

SL machines could potentially offer significant advantages in both the processing of and training on big data sets at high speeds. For example, optical SL machines would benefit from high parallelism and fast all-optical nonlinearities. A photonic circuit with L layers and N -dimensional inputs would be able to perform a full HEB step at once (forward and backward pass) that is equivalent to $\mathcal{O}(LN^2)$ operations on a digital computer. The rate of training steps would be constrained by the latency per layer of the circuit (because two pulses cannot be inside at the same time), and the time required to implement a time reversal. The speed of the time-reversal operation is limited by the response time of the Kerr nonlinearity, which can be on the order of 100fs [27]. Using a conservative estimate of the length of the layers on the order of 1mm, the latency would be less than 10ps. Therefore, a conventional computer would have to perform on the order of $N^2 10^{11}$ multiply-accumulate (MAC) operations per second in order to match an optical SL machine. Furthermore, in many big-data applications, the real bottleneck in the speed of training is in the RAM bandwidth. For large ANN's, storing or retrieving the updated weights at each step can be the most important contribution to the training time. That is possibly one of the biggest advantages of the SL machines: the memory (the learning field) is updated at the same time that the evaluation field propagates in the device, so there is no overhead associated to memory retrieval.

Another potential advantage is energy efficiency. It has been suggested that optical neural networks [10] can be orders of magnitude more efficient in terms of power than their electronic counterparts. Moreover, we shall remark that there is no loss during the time-reversible Hamiltonian evolution in a SL machine. Therefore, all the power consumption comes from: (1) preparing the

input and injecting the error signal, (2) time-reversing the output, and (3) the decay step. A calculation of the power consumption would depend on the details of the particular implementation, but since the matrix multiplications and nonlinear activation functions are realized in the time-reversible lossless step, it is reasonable to expect a better energy efficiency than current electronic hardware.

VIII. CONCLUSIONS

In this work we have introduced a general method, Hamiltonian Echo Backpropagation, to train SL machines based on Hamiltonian physical systems. For any physical device that meets some general assumptions, our method is guaranteed to realize gradient descent optimization of a cost function. The HEB procedure updates the learning parameters autonomously and *in situ*, leveraging all the advantages of a neuromorphic device. Whether the physical device could achieve a good performance on a particular task will depend on its size and its expressive power, but our method can always find a local minimum of the cost function via physical dynamics. Our numerical simulations illustrate how it can be applied both to simple physical systems and also to other more sophisticated architectures. In fact, we showed an example of its application in the case of a photonic convolutional neural network used for image recognition. Although there are many previous proposals and even experimental implementations of photonic learning machines, most of their potential advantages cannot be leveraged without a training method that is fully autonomous. We believe that when HEB is directly applied to such photonic devices, this will greatly enhance their capabilities.

Going beyond the realm of photonics, there are many other promising physical platforms for machine learning hardware. To name a few, spin devices, clouds of cold atoms or superconducting microwave circuits are examples of nonlinear physical systems where a backpropagation scheme has not been realized yet. We believe that our method would be especially helpful when there is no control over the internal dynamics of the device. Indeed, since none of the steps in HEB depend on the underlying Hamiltonian, one can use the physical device as a black box. Our method not only allows to consider various physical platforms, it will also make easier to explore new architectures. As opposed to other previous proposals, HEB does not rely on a sequential multi-layered structure, which means that it can be used to train new architectures going beyond the structure of a standard ANN.

Appendix A EXAMPLE: XOR FUNCTION

The first example of a SL machine that we show has a particularly simple architecture. The evaluation dynamical variable is a nonlinear wave field propagating in a 2D square lattice. We consider a tight-binding model with hard-wall boundary conditions in which every node of the lattice is coupled to its nearest neighbours. At each site of the lattice there is a nonlinear attractive Kerr self-interaction. The learning dynamical variable is given by another field that does not propagate. We assume that the learning field and the evaluation field interact through a term in the Hamiltonian given by $\theta\Psi^*\Psi$, which is the simplest term that can produce local phase shifts.

During the time-reversible steps, the equations of motion for both fields are given by

$$i\dot{\Psi} = \frac{\beta}{2}\nabla^2\Psi + (\chi\theta + g|\Psi|^2)\Psi, \quad (26)$$

$$i\dot{\theta} = i\Omega\pi_\theta + \chi|\Psi|^2. \quad (27)$$

The hard-wall boundary conditions are given by $\Psi(x=0, z) = \Psi(x=W, z) = \Psi(x, z=0) = \Psi(x, z=L) = 0$.

During the decay step, the evolution of θ is given by $\dot{\theta} = \Omega\pi_\theta$, $\dot{\pi}_\theta = -\Gamma\pi_\theta$.

The goal of this example is to learn a simple logical function. In particular, we choose the XOR function, $b = a_1 \oplus a_2$, since it is well known that it cannot be learned by a single-layer perceptron. For each logical input, (a_0, a_1) , we provide a physical input as a superposition of wave packets, $\Psi(\mathbf{x}, -T) = f^0(\mathbf{x}, a_0) + f^1(\mathbf{x}, a_1)$. Each wave packet, $f^s(\mathbf{x}, a_s)$, is a gaussian wave packet centered around $((2s+1)W/8 + a_s W/2, l_{in})$, $s \in \{0, 1\}$ whose standard deviation is given by σ . In addition, each wave packet has an initial positive momentum in the propagation direction. In this way, each input boolean variable a_s is encoded in the position of the center of the corresponding wave packet.

We train such a self-learning machine to learn the XOR function using Hamiltonian echo back-propagation. The cost function is given by

$$C := \int dx dz \phi(\mathbf{x}) |\Psi(\mathbf{x}, 0) - \Psi_{tar}(\mathbf{x}, b)|^2, \quad (28)$$

where $\phi(\mathbf{x}, b) = \frac{1}{2\pi\sigma_\phi^2} \cdot \sum_{j=0}^1 e^{-(\mathbf{x}-\mathbf{x}_j^{out})^2/(2\sigma_\phi^2)}$ is a sum of two Gaussian functions centered around $\mathbf{x}_0^{out} = (w, 0.8L)$ and $\mathbf{x}_1^{out} = (3w, 0.8L)$, respectively. The target field, $\Psi_{tar}(\mathbf{x}, b)$, is also a Gaussian function centered around \mathbf{x}_b^{out} . Therefore, our cost function is a version of the MSE weighted by $\phi(\mathbf{x})$. In this way, the SL machine tries to fit $\Psi(\mathbf{x}, 0)$ to $\Psi_{tar}(\mathbf{x})$ inside the peaks of $\phi(\mathbf{x})$, where the output is measured. We finally evaluate the accuracy by the following prescription: if $|\Psi(\mathbf{x}_0^{out}, 0)| > |\Psi(\mathbf{x}_1^{out}, 0)|$, the logical output is 0; otherwise it is 1.

In order to solve numerically the equations of motion for the time-reversible steps, we used a split-step method. In particular, we used the symmetrized Fourier split step method, which takes half a time step using the linear operator in momentum space, then takes a full-time step with the nonlinear operator in position space, and then takes a second half time step again with the linear operator in momentum space. In order to satisfy hard wall boundary conditions, the discrete sine transform was used. We approximate the effect of the cost function perturbation by a single small Euler step at $t=0$ (this is a reasonable approximation when ϵ is small enough). For the decay step, we assumed that we are in the regime in which Eq.(6) applies. Therefore, for each HEB step we simulate a forward pass, a backward pass and then we update the parameters according to Eq.(6).

We used a square lattice with 50×150 sites. The nonlinear strength was chosen as $g = 10^2 I^{-1} T^{-1}$, where $I := (2\sigma)^{-2} \int dx dz |\Psi|^2$ is a measure of the peak intensity of the input field. In this way, the accumulated phase shift due to the nonlinear self-interaction is much larger than 2π . The dispersion coefficient has to be large enough to prevent a self-focusing collapse. This implies that $\frac{\beta}{2}\nabla^2\Psi$ should be at least on the same order as $g|\Psi|^2\Psi$. In our numerical simulation, we set $\beta = 10^2 \frac{(2\sigma)^2}{T}$. With this choice of parameters, one can check in the numerical simulations that the extent of the wave packets remains in the order of $(2\sigma)^2$ during the whole forward pass. We choose the initial momentum of the wave packets as $k_z = \frac{3}{4} \frac{L}{T\beta}$, so that they propagate a distance $3L/4$ during the forward pass.

The parameter Ω determines the rate of change of θ . In order to have results that can be more easily interpreted, we work in the regime in which θ remains almost constant during a single forward pass. Hence, we choose $\Omega = 10^{-2}T$. Next, we must choose Γ so that $\frac{\Omega}{\Gamma} \gg \frac{\partial C}{\partial \pi_\theta(-T)} \left(\frac{\partial C}{\partial \theta(-T)} \right)^{-1}$, if we want to work in the regime in which Eq.(6) applies. Since the cost function depends on π_θ only indirectly, through the evolution of θ , one can estimate that $\frac{\partial C}{\partial \pi_\theta(-T)}$ is on the order of $\Omega T \frac{\partial C}{\partial \theta(-T)}$. Hence, we must make sure that $1/\Gamma \gg T$. In particular, we set $\Gamma = 10^{-2}T$. After one training step, the update in θ is of the order of $\epsilon \frac{\Omega}{\Gamma} \chi I$. Hence, the change in the phase shift in Ψ due to the interaction with θ is in the order of $\epsilon \frac{\Omega}{\Gamma} \chi^2 IT$. On the one hand, this update must be small enough so that the stochastic gradient descent works. On the other hand, it should not be so small that the training progress is too slow. We choose $\chi = 10^2 \left(\frac{\Omega}{\Gamma \epsilon IT} \right)^{1/2}$. In our numerical simulations, we set $I = 1$, $T = 1$, $L = 3$, $\sigma = 0.1$.

Appendix B EXAMPLE: IMAGE RECOGNITION

As an illustrative example of a SL machine, we considered a device based on a photonic neural network proposed by Ong et al [31], thereby showing how an existing device design can profit from our self-learning procedure. It is composed of three convolutional layers followed by a dense fully-connected layer. The nonlinearity is provided by a $\chi^{(2)}$ optical nonlinearity, as described in Eq. (22). Both the convolutional layers and the fully connected layer can be implemented by a sequence of discrete Fourier transforms (DFTs) and learnable phase shifts. In Ong et al., the activation function is a complex version of the ReLU function. Instead, we choose the activation function given by a $\chi^{(2)}$ nonlinear interaction, which in principle can be implemented in a physical setup. As a cost function, we choose the mean square error on the intensity.

The processing inside the photonic convolutional neural network that we consider is composed of a sequence of operations acting on a 2D square grid of $N \times N$ modes. In addition to the evaluation modes, there are learning and ancillary modes that take part in the sequential operations and also have to be time-reversed.

Any convolution (with periodic boundary conditions) is diagonalized by the DFT. Therefore, the weight matrix in a convolutional layer can be performed by applying a DFT, then a diagonal matrix, and finally the inverse DFT. In the case of a unitary convolution, the diagonal matrix is of the form $D_{jj} = e^{i\theta_j}$ (i.e., a phase mask). All these three operations are unitary operations that can be implemented with a lossless photonic circuit. The DFT matrix is of course fixed; all the learning parameters, θ_j , are contained in the phase mask.

The last two layers of the network are fully connected, and they should be able to express any arbitrary complex matrix. The implementation of these fully connected layers was not described in [31], so we provide a possible version here. We use a decomposition based on the singular value decomposition. In the singular value decomposition, any complex matrix can be cast as a product of the form USV , where U , V are unitary matrices and S is a diagonal matrix. The unitary matrices can always be expressed as a product of the form $U = D_0 \prod F D_i$, where F are DFT matrices and D_i are diagonal unitary matrices (phase masks) [36]. Finally, the singular value matrix, S , can be implemented by means of a linear interaction with an ancilla, provided that the singular values are bounded by $S_{ii} \leq 1$. This is achieved by coupling every relevant mode to an ancilla mode by a means of a general $SU(2)$ linear transformation, when the ancilla is initially zero. Any such transformation can be achieved by means of the product of a 50-50 beam-splitter, a phase shift, and another 50-50 beam-splitter. Since an overall scaling factor in the weight matrix is unimportant, it is sufficient that our implementation can produce any complex matrix with $|S_{ii}| \leq 1$.

All the trainable parameters are contained in the phase shifts, which in this example are realized by a local interaction Hamiltonian given by $\theta\Psi^*\Psi$. Just like in the first example, we assume that the machine operates in the limit in which the dissipation time-scale is much longer than the duration of a forward pass.

For the numerical implementation, we solved the evolution of the evaluation and learning fields in a sequential manner. There are three kinds of operations inside each forward pass: (1) DFT's, (2) the interaction of Ψ and Θ , (3) the interaction of Ψ and Ψ_{anc} (the ancilla in the dense layers), (4) the nonlinear activation function, and (5) the cost function perturbation. Each of these steps represents a different layer in the photonic device, and therefore they can be solved separately. The 2D DFT was performed by means of a fast Fourier transform algorithm. The step (2) corresponds to the interaction described by the Hamiltonian $H = \chi_l \theta \Psi^* \Psi$. The equations of motion for this step can easily be solved analytically. Therefore, we can calculate the overall effect of the step (2) by means of a simple formula. In the same way, the step (3) is described by the Hamiltonian $H = J(\Psi^* \Psi_{anc} + \Psi \Psi_{anc}^*)$, which can also be solved analytically. The step (4) is integrable too, with the solution given by Eq.(22). The step (5) is a small perturbation that can be well approximated by a single Runge-Kutta step. For the backward, pass, the same operations are performed, but starting with the phase conjugation of the output of the forward pass. Of course, one has to time-reverse not only the evaluation field, but also all the ancillary and learning variables.

The photonic convolutional neural network that we considered has three convolutional layers and two fully connected layers. The convolutional layers are somewhat unconventional: they only have one filter, but it has the same size of the output. As we already described, this is accomplished by an alternation of a DFT, a phase mask and another DFT. The first DFT acts on the full input image with N^2 modes, while the phase mask and the second DFT act only on the innermost M^2 modes. The rest of the modes are considered to be ancillary modes. In particular, the first layer has $(N, M) = (31, 31)$, the second has $(N, M) = (31, 21)$, and the third has $(N, M) = (21, 17)$. The size of the input and output of the fully connected layers are $(17, 9)$ and $(9, 4)$, respectively. The input of the network is a rescaled version of the corresponding image from MNIST. The intensity of the field at each input mode goes from 0 to I_{max} (which has units of the square root of an action). In the numerical simulation, we set $I_{max} = 1$. Also, we set that all the elementary steps (activation functions, interaction with θ , etc.) have duration $T_s = 1$. At the convolutional and dense layers we have two different values of the nonlinear strength, which are given by χ_1 and χ_2 respectively. From Eq.(22) one can deduce that both χ_1 and χ_2 have to be chosen so that $\chi_i |\Psi| T_s \approx 1$ for the dynamics to be strongly nonlinear. The nonlinear strength was chosen as described in figure 7. The coupling to the ancilla is given by $J = 10^1 T_s^{-1}$, since we want

to ensure that the mixing of the ancilla and the relevant modes is on the order of 1.

With regard to the decay step, it is assumed that we are in the regime in which Eq.(6) applies. Therefore, for each HEB step we simulate a forward pass, a backward pass and then we update the parameters according to Eq.(6). The coefficient of the cost function perturbation

is taken to be $\epsilon = 10^{-2}$, and we set $\Omega = 10^{-1}T^{-1}$ so that the update of θ during a single forward pass can be neglected. We use a damping coefficient given by $\Gamma = 10^{-1}T^{-1}$ so that the learning rate is given by $\eta = 10^{-2}T$. Finally, by a similar argument to the learning of the XOR function, we set $\chi_l = 10^1 \left(\frac{\Omega}{\Gamma \epsilon I_{max} T} \right)^{1/2}$ (see Appendix A).

-
- [1] I. Goodfellow, Y. Bengio, and A. Courville, *Deep Learning* (MIT Press, 2016), <http://www.deeplearningbook.org>.
- [2] C. D. Schuman, T. E. Potok, R. M. Patton, J. D. Birdwell, M. E. Dean, G. S. Rose, and J. S. Plank, arXiv:1705.06963 [cs] (2017), arXiv: 1705.06963, URL <http://arxiv.org/abs/1705.06963>.
- [3] B. J. Shastri, A. N. Tait, T. Ferreira de Lima, W. H. P. Pernice, H. Bhaskaran, C. D. Wright, and P. R. Prucnal, *Nature Photonics* **15**, 102 (2021), ISSN 1749-4885, 1749-4893, URL <http://www.nature.com/articles/s41566-020-00754-y>.
- [4] K. Wagner and D. Psaltis, *Applied Optics* **26**, 5061 (1987), ISSN 0003-6935, 1539-4522, URL <https://www.osapublishing.org/abstract.cfm?URI=ao-26-23-5061>.
- [5] K. Wagner and T. M. Slagle, *Applied Optics* **32**, 1408 (1993), ISSN 0003-6935, 1539-4522, URL <https://www.osapublishing.org/abstract.cfm?URI=ao-32-8-1408>.
- [6] D. E. Rumelhart, G. E. Hinton, and R. J. Williams, *Nature* **323**, 533 (1986), ISSN 0028-0836, 1476-4687, URL <http://www.nature.com/articles/323533a0>.
- [7] D. Psaltis, D. Brady, and K. Wagner, *Applied Optics* **27**, 1752 (1988), ISSN 0003-6935, 1539-4522, URL <https://www.osapublishing.org/abstract.cfm?URI=ao-27-9-1752>.
- [8] G. Wetzstein, A. Ozcan, S. Gigan, S. Fan, D. Englund, M. Soljačić, C. Denz, D. A. B. Miller, and D. Psaltis, *Nature* **588**, 39 (2020), ISSN 0028-0836, 1476-4687, URL <http://www.nature.com/articles/s41586-020-2973-6>.
- [9] J. Feldmann, N. Youngblood, C. D. Wright, H. Bhaskaran, and W. H. P. Pernice, *Nature* **569**, 208 (2019), ISSN 0028-0836, 1476-4687, URL <http://www.nature.com/articles/s41586-019-1157-8>.
- [10] Y. Shen et al., *Nature Photonics* **11**, 441 (2017), ISSN 1749-4885, 1749-4893, arXiv: 1610.02365, URL <http://arxiv.org/abs/1610.02365>.
- [11] X. Guo, T. D. Barrett, Z. M. Wang, and A. I. Lvovsky, arXiv:1912.12256 [physics] (2020), arXiv: 1912.12256, URL <http://arxiv.org/abs/1912.12256>.
- [12] S. R. Skinner, E. C. Behrman, A. A. Cruz-Cabrera, and J. E. Steck, *Applied Optics* **34**, 4129 (1995), ISSN 0003-6935, 1539-4522, URL <https://www.osapublishing.org/abstract.cfm?URI=ao-34-20-4129>.
- [13] H.-Y. S. Li, Y. Qiao, and D. Psaltis, *Applied Optics* **32**, 5026 (1993), ISSN 0003-6935, 1539-4522, URL <https://www.osapublishing.org/abstract.cfm?URI=ao-32-26-5026>.
- [14] S. Hu, Y. Liu, Z. Liu, T. Chen, J. Wang, Q. Yu, L. Deng, Y. Yin, and S. Hosaka, *Nature Communications* **6** (2015), ISSN 2041-1723, URL <http://www.nature.com/articles/ncomms8522>.
- [15] D. Soudry, D. Di Castro, A. Gal, A. Kolodny, and S. Kvatinsky, *IEEE Transactions on Neural Networks and Learning Systems* **26**, 2408 (2015).
- [16] A. Sengupta and K. Roy, in *2015 International Joint Conference on Neural Networks (IJCNN)* (IEEE, Killarney, Ireland, 2015), pp. 1–7, ISBN 978-1-4799-1960-4, URL <http://ieeexplore.ieee.org/document/7280306/>.
- [17] J. Grollier, D. Querlioz, and M. D. Stiles, *Proceedings of the IEEE* **104**, 2024 (2016).
- [18] M. Hermans, M. Burm, T. Van Vaerenbergh, J. Dambre, and P. Bienstman, *Nature Communications* **6** (2015), ISSN 2041-1723, URL <http://www.nature.com/articles/ncomms7729>.
- [19] K. W. Hughes, M. Minkov, Y. Shi, and S. Fan, *Optica* **5**, 864 (2018), ISSN 2334-2536, URL <https://www.osapublishing.org/abstract.cfm?URI=optica-5-7-864>.
- [20] I. Stakgold and M. Holst, eds., *Green's Functions and Boundary Value Problems* (John Wiley and Sons, Inc., Hoboken, NJ, USA, 2011), ISBN 978-0-470-90653-8 978-0-470-60970-5, URL <http://doi.wiley.com/10.1002/9780470906538>.
- [21] D. A. B. Miller, *Optics Letters* **5**, 300 (1980), ISSN 0146-9592, 1539-4794, URL <https://www.osapublishing.org/abstract.cfm?URI=ol-5-7-300>.
- [22] T. W. Hughes, I. A. D. Williamson, M. Minkov, and S. Fan, *Science Advances* **5**, eaay6946 (2019), ISSN 2375-2548, URL <https://advances.sciencemag.org/lookup/doi/10.1126/sciadv.aay6946>.
- [23] M. Reck, A. Zeilinger, H. J. Bernstein, and P. Bertani, *Physical Review Letters* **73**, 58 (1994), ISSN 0031-9007, URL <https://link.aps.org/doi/10.1103/PhysRevLett.73.58>.
- [24] N. J. Doran and D. Wood, *Optics Letters* **13**, 56 (1988), ISSN 0146-9592, 1539-4794, URL <https://www.osapublishing.org/abstract.cfm?URI=ol-13-1-56>.
- [25] M. Soljačić, M. Ibanescu, S. G. Johnson, Y. Fink, and J. D. Joannopoulos, *Physical Review E* **66** (2002), ISSN 1063-651X, 1095-3787, URL <https://link.aps.org/doi/10.1103/PhysRevE.66.055601>.
- [26] M.-S. Kang, J. Heo, S.-G. Choi, S. Moon, and S.-W. Han, *Scientific Reports* **10**, 5123 (2020), ISSN 2045-2322, URL <https://doi.org/10.1038/s41598-020-61938-8>.
- [27] R. W. Boyd, *Nonlinear Optics, Third Edition* (Academic Press, Inc., USA, 2008), 3rd ed., ISBN 0123694701.
- [28] G. He, *Progress in Quantum Electronics* **26**, 131 (2002), ISSN 00796727, URL <https://linkinghub.elsevier.com/retrieve/pii/S0079672702000046>.

- [28] A. V. Sharypov, X. Deng, and L. Tian, *Phys. Rev. B* **86**, 014516 (2012), URL <https://link.aps.org/doi/10.1103/PhysRevB.86.014516>.
- [29] J. Martin, B. Georgeot, and D. L. Shepelyansky, *Physical Review Letters* **101** (2008), ISSN 0031-9007, 1079-7114, URL <https://link.aps.org/doi/10.1103/PhysRevLett.101.074102>.
- [30] T. Inagaki, Y. Haribara, K. Igarashi, T. Sonobe, S. Tamate, T. Honjo, A. Marandi, P. L. McMahon, T. Umeki, K. Enbutsu, et al., *Science* **354**, 603 (2016), ISSN 0036-8075, 1095-9203, URL <http://www.sciencemag.org/cgi/doi/10.1126/science.aah4243>.
- [31] J. R. Ong, C. C. Ooi, T. Y. L. Ang, S. T. Lim, and C. E. Png, *IEEE Journal of Selected Topics in Quantum Electronics* **26**, 1 (2020), ISSN 1077-260X, 1558-4542, URL <https://ieeexplore.ieee.org/document/9049096/>.
- [32] G. Marcucci, D. Pierangeli, and C. Conti, *Physical Review Letters* **125** (2020), ISSN 0031-9007, 1079-7114, URL <https://link.aps.org/doi/10.1103/PhysRevLett.125.093901>.
- [33] P. Crotty, D. Schult, and K. Segall, *Physical Review E* **82** (2010), ISSN 1539-3755, 1550-2376, URL <https://link.aps.org/doi/10.1103/PhysRevE.82.011914>.
- [34] Q. Wang, A. Hamadeh, R. Verba, V. Lomakin, M. Mohseni, B. Hillebrands, A. V. Chumak, and P. Pirro, *npj Computational Materials* **6** (2020), ISSN 2057-3960, URL <http://www.nature.com/articles/s41524-020-00465-6>.
- [35] Y. Yamamoto, K. Aihara, T. Leleu, K.-i. Kawarabayashi, S. Kako, M. Fejer, K. Inoue, and H. Takesue, *npj Quantum Information* **3** (2017), ISSN 2056-6387, URL <http://www.nature.com/articles/s41534-017-0048-9>.
- [36] V. J. López-Pastor, J. S. Lundeen, and F. Marquardt, arXiv:1912.04721 [physics, physics:quant-ph] (2019), arXiv: 1912.04721, URL <http://arxiv.org/abs/1912.04721>.